おわりに

著者らは，グルタミン酸の細胞外濃度を制御するグルタミン酸トランスポーターGLAST，GLT1の機能を阻害したマウスを作製し，そのマウスに社会性行動の異常・繰り返し行動・統合失調症の陰性症状や陽性症状に相当する行動異常が起こることを発見した．また，これらのマウスに，細胞種特異的な神経細胞死が起こることを見出した．さらに，統合失調症・うつ病・強迫性障害・筋萎縮性側索硬化症・ハンチントン病・アルツハイマー病・緑内障などさまざまな精神神経疾患において，グリア型グルタミン酸トランスポーターの異常が報告されている．

グリア型グルタミン酸トランスポーターの機能障害は，どのようにして神経細胞死および神経細胞の形成・機能障害をもたらすのか？現在までわかっている機序としては，以下の三つが考えうる（**図1**）．1）細胞外グルタミン酸濃度の上昇によるシナプス外グルタミン酸受容体および隣接シナプスのグルタミン酸受容体の活性化，2）グリア内グルタミン酸の枯渇がもたらすグルタチオン合成の減少による酸化ストレスの亢進，3）神経活動が亢進している部位への選択的エネルギー補給システムの障害[16]．

著者らは，さまざまな精神神経疾患の中に，グルタミン酸トランスポーターの異常が原因で発症する患者が一定の割合存在し，「グルタミン酸トランスポーター機能異常症候群」として分類できると考えている．グルタミン酸トランスポーター機能異常症候群の患者には，グルタミン酸トランスポーターの取り込み活性を促進する薬物が，共通した治療薬として有効であると期待される[17]．

参考文献

1) Nakanishi S, et al : Glutamate receptors: brain function and signal transduction. Brain Res Rev **26** : 230-235, 1998.
2) Choi DW : Glutamate neurotoxicity and diseases of the nervous system. Neuron **1** : 623-634, 1988.
3) Patil ST, et al : Activation of mGluR2/3 receptors as a new approach to treat schizophrenia: a randomized Phase 2 clinical trial. Nat Med **13** : 1102-1107, 2007.
4) Walsh T, et al : Rare structural variants disrupt multiple genes in neurodevelopmental pathways in schizophrenia. Science **320** : 539-543, 2008.
5) Need AC, et al : Exome sequencing followed by large-scale genotyping suggests a limited role for moderately rare risk factors of strong effect in schizophrenia. Am J Hum Genet **91** : 303-312, 2012.
6) Karlsson RM, et al : Loss of glial glutamate and aspartate transporter (excitatory amino acid transporter 1) causes locomotor hyperactivity and exaggerated responses to psychotomimetics: rescue by haloperidol and metabotropic glutamate 2/3 agonist. Biol Psychiatry **64** : 810-814, 2008.
7) Karlsson RM, et al : Assessment of glutamate transporter GLAST (EAAT1)-deficient mice for phenotypes relevant to the negative and executive/cognitive symptoms of schizophrenia. Neuropsychopharmacology **34** : 1578-1589, 2009.
8) Matsugami TR, et al : Indispensability of glutamate transporters GLAST and GLT1 to brain development. Proc Natl Acad Sci USA **103** : 12161-12166, 2006.
9) Aida T, et al : Overstimulation of NMDA receptors impairs early brain development in vivo. PloS One **7** : e36853, 2012.
10) Schobel SA, et al : Imaging patients with psychosis and a mouse model establishes a spreading pattern of hippocampal dysfunction and implicates glutamate as a driver. Neuron **78** : 81-93, 2013.
11) Ting JT, Feng G : Glutamatergic Synaptic Dysfunction and Obsessive-Compulsive Disorder. Curr Chem Genomics **2** : 62-75, 2008.
12) The Autism Genome Project Consortium : Mapping autism risk loci using genetic linkage and chromosomal rearrangements. Nat Genet **39** : 319-328, 2007.
13) Chen KH, et al : Disturbed neurotransmitter transporter expression in Alzheimer's disease brain. J Alzheimers Dis **26** : 755-766, 2011
14) Mookherjee P, et al : GLT-1 loss accelerates cognitive deficit onset in an Alzheimer's disease animal model. J Alzheimers Dis **26** : 447-455, 2011.
15) Harada T, et al : The potential role of glutamate transporters in the pathogenesis of normal tension glaucoma. J Clin Invest **117** : 1763-1770, 2007.
16) Voutsinos-Porche B, et al : Glial glutamate transporters mediate a functional metabolic crosstalk between neurons and astrocytes in the mouse developing cortex. Neuron **37** : 275-286, 2003.
17) Tanaka K : Antibiotics rescue neurons from glutamate attack. Trends Mol Med **11** : 259-262, 2005.

Development, Growth & Differentiation
The Japanese Society of Developmental Biologists

Develop. Growth Differ. (2014) **56**, 34–45 doi: 10.1111/dgd.12101

Review Article

Translating human genetics into mouse: The impact of ultra-rapid *in vivo* genome editing

Tomomi Aida,[1] Risa Imahashi[1] and Kohichi Tanaka[1,2,3]*

[1]*Laboratory of Molecular Neuroscience, Medical Research Institute, Tokyo Medical and Dental University, 1-5-45, Yushima, Bunkyo-Ku, Tokyo, 113-8510,* [2]*The Center for Brain Integration Research, Tokyo Medical and Dental University, 1-5-45, Yushima, Bunkyo-Ku, Tokyo, 113-8510, and* [3]*JST, CREST, 4-1-8, Honcho, Kawaguchi-shi, Saitama, 332-0012, Japan*

Gene-targeted mutant animals, such as knockout or knockin mice, have dramatically improved our understanding of the functions of genes *in vivo* and the genetic diversity that characterizes health and disease. However, the generation of targeted mice relies on gene targeting in embryonic stem (ES) cells, which is a time-consuming, laborious, and expensive process. The recent groundbreaking development of several genome editing technologies has enabled the targeted alteration of almost any sequence in any cell or organism. These technologies have now been applied to mouse zygotes (*in vivo* genome editing), thereby providing new avenues for simple, convenient, and ultra-rapid production of knockout or knockin mice without the need for ES cells. Here, we review recent achievements in the production of gene-targeted mice by *in vivo* genome editing.

Key words: clustered, regularly interspaced, short palindromic repeats- associated endonuclease, genome editing, mouse, transcription activator-like effector nucleases, zinc-finger nucleases.

Introduction

The mouse has become the most commonly used animal model system in the biological and medical sciences because its genome can be specifically and precisely modified as desired (Capecchi 2005). The invaluable advantage of the mouse is the ability to perform homologous recombination in embryonic stem (ES) cells, an essential step in gene targeting and a technology that was unavailable in the majority of other mammalian species. Since the first success of gene targeting in mouse, thousands of mice, mainly knockout mice created by insertion of a selection marker or reporter into a target gene locus, have been created, unveiling the *in vivo* functions of the genes. As an extension of these efforts, large-scale international consortia were organized to provide knockout mice for all protein-coding genes and systematically analyze the resulting phenotypes (Sung *et al.* 2012; Menke 2013). The International Knockout Mouse Consortium (IKMC) released targeted ES cell lines, including knockout, conditional, and gene-trapped alleles, for more than 18 000 genes, in addition to mice targeted for over 2600 loci (Skarnes *et al.* 2011). Further, the Sanger Institute Mouse Genetics Project (MGP), a founding member of the International Mouse Phenotyping Consortium (IMPC), recently released pilot data from a large-scale systematic phenotype analysis of 489 knockout mouse strains, derived from more than 900 IKMC knockout ES cell lines (White *et al.* 2013). Surprisingly, unbiased screening by the MGP identified many previously unknown phenotypes in both new knockout mice and strains that were the subject of earlier reports. The IMPC will expand this phenotypic screening to cover 5000 knockout mouse lines over the next 4 years and to all 20 000 protein-coding genes in the future. These genome-wide and large-scale systematic knockout mouse resources are now publicly available; thus, researchers can focus their efforts on the detailed functional analysis of genes of interest, rather than on the construction of mouse lines.

Recent advances in genomic microarray and next generation sequencing technologies have revealed the landscape of human genetic diversity, which comprises tens of millions of common and rare variants associated with health and disease (Raychaudhuri 2011; 1000 Genomes Project Consortium *et al.* 2012). Although large-scale genome-wide association studies

*Author to whom all correspondence should be addressed.
Email: tanaka.aud@mri.tmd.ac.jp
Received 20 September 2013; revised 9 October 2013; accepted 10 October 2013.

(GWAS), based on high-density genomic microarray technology, have identified hundreds of frequent variants associated with common and complex human diseases and traits, the majority of these are responsible for only a small amount of the disease risk (Manolio *et al.* 2009). In contrast, with recent advances in unbiased whole-genome and whole-exome sequencing approaches, inherited and rare *de novo* single nucleotide variants (SNVs) are now also believed to be important in common and complex diseases (Cirulli & Goldstein 2010; Veltman & Brunner 2012). The best examples are large-scale exome sequencing studies on hundreds of patient-parent trios or quartets for autism spectrum disorders (ASDs), which are neurodevelopmental conditions characterized by impairments in social interaction and stereotyped behaviors with a strong genetic component (Iossifov *et al.* 2012; Neale *et al.* 2012; O'Roak *et al.* 2012; Sanders *et al.* 2012). These studies consistently report higher rates of *de novo*, especially nonsense, splice site, or frameshift SNVs in patients with ASD than in their unaffected siblings (Veltman & Brunner 2012). Further, they also unveiled extreme genetic heterogeneity in ASD, as evidenced by the uncovering of *de novo* SNVs in hundreds of different genes in different individuals. This indicates the need for further efforts to investigate the biological consequences of these rare *de novo* SNVs (Veltman & Brunner 2012).

One possible approach to address the biological function of these SNVs, as well as determining whether they are causal for the human phenotype of interest, is the use of genetic mouse models incorporating the identified variants. Precisely modified knockin mouse models carrying such human SNVs provide a unique and direct approach for the investigation of the functional consequence of variants *in vivo*. Pioneer work in this field by Südhof and colleagues reported that a knockin mouse carrying a neuroligin-3 R451C SNV found in a subset of ASD patients exhibited abnormal behaviors that resembled those of human patients, in addition to abnormal synaptic transmission (Tabuchi *et al.* 2007). Importantly, in contrast to R451C knockin mouse, neuroligin-3 knockout mouse did not exhibit such abnormalities, suggesting that the R451C SNV represents a gain-of-function mutation (Tabuchi *et al.* 2007). Similarly, in Rett syndrome, an ASD caused by mutations in methyl-CpG-binding protein 2 (MeCP2), many SNVs throughout the *MECP2* gene were identified and several knockin mouse lines carrying each SNV provided important insights into the biological and phenotypic significance of each variant, as well as identifying downstream targets of MeCP2 (Tao *et al.* 2009; Jentarra *et al.* 2010; Cohen *et al.* 2011; Goffin *et al.* 2011; Ebert *et al.* 2013; Lyst *et al.* 2013). Taken together these studies demonstrate that mouse models for human SNVs, rather than simple knockout mice, are essential and extremely valuable tools for the biological and phenotypic interpretation of human variants and the development of novel treatments.

Although the demand for precisely modified knockin mouse models carrying human SNVs is growing, a recent review by Menke reported that only 600 such mice could be found in the Mouse Genome Informatics database (Menke 2013). This is partially due to the difficulty of generating such mice by conventional gene targeting technology using homologous recombination in ES cells; a time-consuming, laborious, and expensive process (Capecchi 2005).

In vivo genome editing in mice

The recent emergence and drastic evolution of genome editing technologies is revolutionizing gene targeting in the mouse (Sung *et al.* 2012; Menke 2013). The methods are based on molecular tools, including zinc-finger nucleases (ZFNs), transcription activator-like effector (TALE) nucleases (TALENs), and clustered, regularly interspaced, short palindromic repeats (CRISPR) and the CRISPR-associated endonuclease (Cas), known as the CRISPR/Cas system. These methods provide exciting and groundbreaking opportunities, enabling direct and rapid gene targeting in fertilized mouse eggs, with no need for ES cells. The basic characteristics and various applications of these genome editing technologies will be discussed by others in this special issue of DGD. Here, we focus on gene targeting in the mouse by *in vivo* genome editing and review current achievements, issues to be solved, and future applications.

The principle of *in vivo* editing involves targeting of the genome by direct microinjection of plasmid DNA or mRNA encoding editing tools (ZFNs, TALENs, or CRISPR/Cas) into the cytoplasm or pronuclei of one-cell embryos to generate a DNA double-strand break (DSB) at a specific target locus (Fig. 1, Urnov *et al.* 2010; Joung & Sander 2013). The DSB is subsequently repaired by two major cellular endogenous DNA damage repair pathways; the error-prone, non-homologous end-joining (NHEJ) route, which results in small deletions or sequence insertions into the DSB site, and the homology-directed repair (HDR) pathway, which relies on a donor DNA template with homology to the DSB site to achieve precise homologous recombination. NHEJ occurs rapidly and preferentially, often leading to frameshift mutations and loss-of-function of the targeted genes, resulting in a knockout mouse when the protein-coding sequence is targeted (Fig. 1,

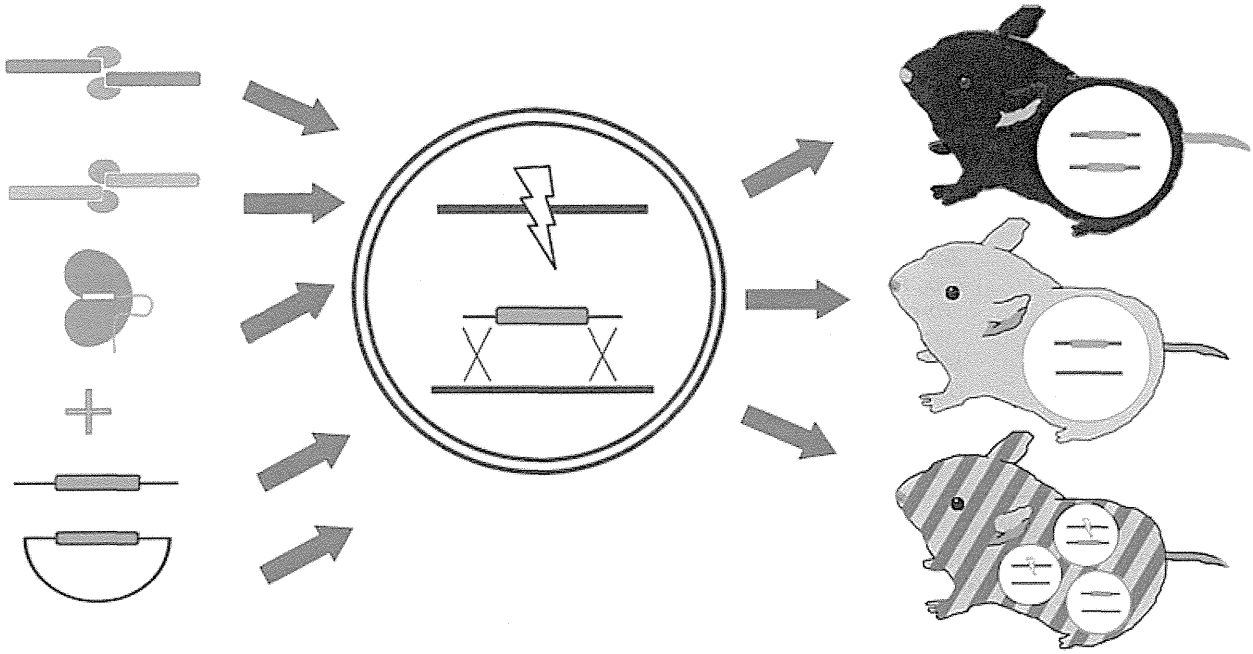

Fig. 1. Schematic diagram of *in vivo* genome editing in mouse. Transcription activator-like effector nucleases (TALENs) (blue), zinc-finger nucleases (ZFNs) (pink), or clustered, regularly interspaced, short palindromic repeats-associated endonuclease (CRISPR/Cas) (green) are microinjected into one-cell fertilized eggs (circle in the middle) derived from wildtype mice with or without ssOligo or targeting vector for knockin mouse production. Then, double-strand break (DSB) and subsequent homology-directed repair (HDR) (red) and/or non-homologous end-joining (NHEJ) (yellow) are induced within one-cell fertilized eggs, resulting in genetically-mosaic (striped), monoallelically-targeted heterozygous (gray-colored), or biallelically-targeted homozygous (black-colored) mutant mice at F0.

Carbery *et al.* 2010; Sung *et al.* 2013; Shen *et al.* 2013; Wang *et al.* 2013a). HDR infrequently occurs and leads to precise and specific genome modifications, such as SNV substitutions, insertions, deletions, or gene replacement, when a targeting vector or synthetic single-strand oligonucleotide (ssOligo) is co-microinjected into mouse embryos, resulting in a knockin mouse (Fig. 1, Meyer *et al.* 2010; Cui *et al.* 2011; Meyer *et al.* 2012; Wefers *et al.* 2013; Wang *et al.* 2013a; Yang *et al.* 2013). A series of groundbreaking successes indicate that *in vivo* genome editing in the mouse is robust and has great potential as an alternative to the conventional gene targeting approach.

Knockout mice

After the first success of NHEJ-mediated gene knockout by *in vivo* genome editing in mammals was achieved in rat with ZFNs targeting three different genes (Geurts *et al.* 2009), it was rapidly applied to mouse (Table 1). Cui and colleagues from Sigma-Aldrich, the exclusive supplier of ZFNs, reported the first knockout mice by *in vivo* genome editing with ZFNs (Carbery *et al.* 2010). They targeted three endogenous genes in both FVB/N and C57BL/6J strains with targeting efficiencies from 20 to 75% of live newborns and no off-target effects at 20 potential sites. The founder mice were heterozygous or genetically mosaic, carried more than one mutant allele, and successfully produced F1 mutant progeny. Importantly, homozygous mice were generated from F1 mutants within 4 months (Fig. 2).

Similar work was performed for the targeting of the *ROSA26* locus, a safe harbor often used for gene targeting (Hermann *et al.* 2012). Although the efficiency in this study was <10%, one of the founders had a biallelic modification, resulting in an F0 biallelic knockout mouse that drastically reduced the time taken to produce homozygous knockouts (Fig. 2).

Although the simple modular DNA recognition code of TALENs and the existence of publicly available resources has resulted in the rapid expansion of TALENs as versatile genome editing tools, the first knockout mice by TALEN-mediated *in vivo* genome editing were reported in 2013 (Sung *et al.* 2013). Two endogenous genes were targeted with efficiencies from 49 to 77% in live newborns with no off-target effects. All alleles present in F0 founders were successfully transmitted to F1 progeny. Importantly, targeting and biallelic modification efficiencies were increased when microinjection was performed with a high dose of TALEN mRNA; when 50 ng/μL of TALEN

Table 1. Summary of non-homologous end-joining (NHEJ) in mice by *in vivo* genome editing

Nucleases	Targets	Genes	NHEJ (%)	Off-target	F1	Refs
ZFNs	3	*Mdr1a, Jag1, Notch3*	19.5–77.3	None	Yes	Carbery *et al.* (2010)
ZFNs	1	*ROSA26*	22.4[†]	n.d.	n.d.	Meyer *et al.* (2010)
ZFNs	1	*Mdr1a*	7.5–75.0[‡]	n.d.	n.d.	Cui *et al.* (2011)
ZFNs	1	*ROSA26*	4.6–8.7[†]	n.d.	n.d.	Hermann *et al.* (2012)
TALENs	2	*Pibf1, Sepw1*	48.7–76.9[†]	None	Yes	Sung *et al.* (2013)
TALENs	1	*Rab38*	2.0–6.0	n.d.	Yes	Wefers *et al.* (2013)
TALENs	1	*Zic2*	10.0–46.7	n.d.	Yes	Davies *et al.* (2013)
TALENs	10	*Lepr, Pak1ip1, Gpr55, Rprm, Fbxo6, Smurf1, Tmem74, Wdr20a, Dcaf13, Fam73a*	12.5–66.7[†]	None[§]	Yes	Qiu *et al.* (2013)
TALENs	1	*Mlkl*	18.2[†]	n.d.	Yes	Wu *et al.* (2013)
TALENs	2	*C9orf72, Fus*	7.5–41.2	None	Yes	Panda *et al.* (2013)
CRISPR/Cas	2	*Pouf5-EGFP, CAG-EGFP*	14.3–20.0	n.d.	n.d.	Shen *et al.* (2013)
CRISPR/Cas	3	*Tet1, Tet2, Tet3*	66.7–100.0[†,¶]	None	n.d.	Wang *et al.* (2013a)
CRISPR/Cas	3	*Th, Rheb, Uhrf2*	75.0–91.7[††]	None	Yes	Li *et al.* (2013)

[†]Including biallelic modification, [‡]mouse data only, [§]for *Smurf1*, [¶]57.8–78.5% for biallelic modification for Tet1 and Tet2, [††]RNA and mouse data only. n.d., not determined. F1 represents germline transmission. Percentages of NHEJ were calculated using the number of NHEJ positive pups as the numerator and the number of the total pups as the denominator. Fetus data were included in some studies.

mRNA targeting the *Pibf1* gene was injected, six of eight F0 founders had biallelic modifications. Similar results were obtained for the *Sepw1* gene, and the absence of Sepw1 protein was confirmed in the biallelically targeted F0 mutants. This work suggests that highly active TALENs are critical for efficient targeting and biallelic modification. Homozygous knockout mice can be generated within 1 month by TALEN-mediated *in vivo* genome editing (Fig. 2).

Since the first report, a flood of knockout mice generated by TALEN-mediated *in vivo* genome editing has been reported. Davies *et al.* (2013) targeted the *Zic2* gene by TALENs in three different mouse strains, including CD1, C3H, and C57BL/6J. Targeting efficiencies producing live newborns or blastocysts varied, with 10%, 23%, and 46% for C57BL/6J, C3H, and CD1, respectively.

Li and colleagues generated a series of knockout mice for 10 genes, revealing the utility, convenience, and robustness of TALEN-mediated *in vivo* genome editing (Qiu *et al.* 2013). Targeting efficiencies varied from 13 to 67%, with an average of 40%, of live newborns. By using one TALEN for the *Lepr* gene, which encodes the Leptin receptor, they showed that there was no difference in the targeting efficiency between two different mouse strains (C57BL/6N and FVB/N).

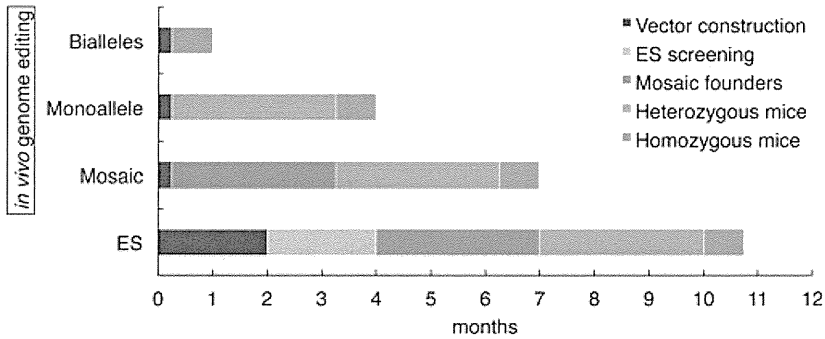

Fig. 2. Time course for homozygous mutant mouse production. ES: embryonic stem (ES)-cell based traditional gene targeting method. Mosaic: genetically-mosaic founders are obtained at F0 by *in vivo* genome editing. Monoallele: monoallelically-targeted heterozygous founders are obtained at F0 by *in vivo* genome editing. Bialleles: biallelically-targeted homozygous founders are obtained at F0 by *in vivo* genome editing. Green: the term to obtain F0 adult mosaic founders from microinjection of genome editing tools, or F0 adult chimeric founders from ES cell microinjection. Orange: the term to obtain adult heterozygous mice from mating of F0 founders with wildtype mice or from microinjection of genome editing tools. Magenta: the term to obtain homozygous newborns from mating of heterozygous mice or from microinjection of genome editing tools. Best cases are shown.

Among the F0 founders, one had biallelic modifications with different frame-shift deletions and exhibited an obese phenotype resembling that of Lepr mutant db/db mice. Further, there were no off-target effects, even at sites with only one mismatch to each TALEN. All the F0 founders tested transmitted the mutant alleles to F1 mice with high efficiency. These results suggest that this method of genome editing is highly accurate and efficient.

Further, Han and colleagues generated knockout mice for *Mlkl* gene (which encodes the mixed lineage kinase domain-like protein, essential for tumor necrosis factor induced necrosis) by TALEN-mediated *in vivo* genome editing (Wu *et al.* 2013). They injected TALEN mRNA into nearly 3000 embryos and obtained 71 mutants from 390 newborns (18% efficiency); of these, four were homozygous mutants.

The latest player, CRISPR/Cas system, is having a drastic impact on the field, due to its simplicity, incredibly high efficiency, and multiplexing capability. Huang and colleagues first generated a knockout mouse in which a green fluorescent protein (GFP) transgene was disrupted by CRISPR/Cas-mediated *in vivo* genome editing (Shen *et al.* 2013). They targeted GFP in two different mouse strains carrying transgenes that encoded GFP, and obtained GFP-deficient mice with targeting efficiencies from 14 to 20% of live newborns.

Next, Jaenisch and colleagues published a revolutionary paper describing the production of mice knocked out for multiple genes with extremely high efficiency (Wang *et al.* 2013a). In this study, they targeted three functionally redundant genes (*Tet1, Tet2, and Tet3*) encoding Ten-eleven translocation (Tet) enzymes that convert 5-methylcytosine to 5-hydroxymethylcytosine. They first investigated the optimal conditions for CRISPR/Cas-mediated *in vivo* genome editing by injecting various amounts (20–200 ng/μL) of Cas9 mRNA, with *Tet1, Tet2* or *Tet3* guide RNAs, into fertilized eggs, and found Cas9 dose-dependent increments in targeting efficiency, with low toxicity in newborn mice. Surprisingly, the vast majority (60–100%) of newborns carried biallelic modifications in each target gene. Further, they simultaneously targeted both *Tet1* and *Tet2*, and obtained double mutants in which all four alleles of these genes were targeted in 80% of newborns without off-target effects. CRISPR/Cas-mediated *in vivo* genome editing can be completed within a month, since construction of CRISPR/Cas vector only takes a few days. This represents an incredible shortcut for the generation of single or double knockout mice, which often takes several years using conventional gene targeting methods (Fig. 2).

Liu and colleagues confirmed the high efficiency of CRISPR/Cas-mediated *in vivo* genome editing (Li *et al.* 2013). They generated three knockout mice targeting *Th, Rheb,* and *Uhrf2*, with targeting efficiencies from 75 to 92% and no off-target effects. They also targeted two adjacent sites, spanning 86 bp, in the *Uhrf2* locus. Importantly, the mutations were successfully transmitted to the next generation, suggesting that the CRISPR/Cas system is the third tool after ZFNs and TALENs to allow heritable *in vivo* genome editing in mice.

Knockin mice

Although the success of *in vivo* genome editing has enabled the rapid generation of knockout mice, developing this technique for the production of knockin mouse models would fully exploit its capabilities (Table 2). In 2010, Kühn and colleagues reported

Table 2. Summary of homology-directed repair (HDR) in mice by *in vivo* genome editing

Nucleases	Targets	Genes	Inserts	Donors	HDR (%)	Off-target	F1	Refs
ZFNs	1	*ROSA26*	*LacZ, Venus*	Plasmid	1.7–4.5	n.d.	n.d.	Meyer *et al.* (2010)
ZFNs	1	*Mdr1a*	*NotI, GFP*	Plasmid	5.0–25.0[†]	n.d.	n.d.	Cui *et al.* (2011)
ZFNs	1	*ROSA26*	*GFP*	Plasmid	2.0	n.d.	Yes	Hermann *et al.* (2012)
ZFNs	1	*Rab38*	*SNV*	Plasmid, ssOligo	1.7–3.5	n.d.	Yes	Meyer *et al.* (2012)
TALENs	1	*Rab38*	*SNV*	Plasmid, ssOligo	0.9–2.0	n.d.	Yes	Wefers *et al.* (2013)
TALENs	1	*Fus*	*SNV*	ssOligo	4.0–8.4	None	Yes	Panda *et al.* (2013)
CRISPR/Cas	2	*Tet1, Tet2*	*EcoRI*	ssOligo	70.0–80.0[‡,§]	None	n.d.	Wang *et al.* (2013a)
CRISPR/Cas	4	*Sox2, Nanog, Oct4, MeCP2*	*V5, mCherry, GFP-Neo, LoxP*	Plasmid, ssOligo	8.1–61.3[¶,††]	Present	n.d.	Yang *et al.* (2013)

[†]Mouse data only, [‡]including biallelic modification, [§]60% for double HDR of both *Tet1* and *Tet2*, [¶]61.3% for loxP site integration, [††]16% for two loxP sites in one allele. n.d., not determined. F1 represents germline transmission. Percentages of HDR were calculated using the number of HDR positive pups as the numerator and the number of the total pups as the denominator. Fetus data were included in some studies.

pioneering work in the production of the first knockin mice using ZFN-mediated *in vivo* genome editing and targeting vectors (Meyer *et al.* 2010). They co-injected mRNAs encoding ZFNs for the *ROSA26* locus and a targeting vector, containing a 4.2 kb *LacZ* reporter cassette, with homology arms flanking the target site of the locus, into one-cell mouse embryos. Fifty-eight embryos were analyzed and one was found to be a precisely modified knockin mouse and was functionally confirmed by X-gal staining. Next, the same ZFN mRNAs were co-injected with a targeting vector containing a 1.1 kb *Venus* reporter cassette, instead of *LacZ.* Among the 22 embryos obtained, they identified one as a precisely modified knockin mouse. The targeting efficiencies of the two experiments were 1.7 and 4.5%, respectively.

Soon afterwards, Cui *et al.* (2011) also reported production of knockin mice and rats with relatively high efficiency. First they tested the targeted integration of a small 8 bp NotI site fragment flanked on each side by 800 bp of homology arms. Co-injection of a targeting vector with ZFNs for two genomic loci (*Mdr1a* and *PXR*) in both rats and mice resulted in knockin mutants with efficiencies of 6.7–25% of embryos. Next, they tested targeted integration of a long DNA fragment using the same donor vector, in which the NotI site was replaced with a 1.5 kb GFP cassette. They injected the GFP vector in the same way as the NotI sequence, and obtained knockin mice and rats for the two genomic loci with efficiencies from 2.4 to 8.3% of embryos or newborns. Further, they confirmed efficient germline transmission in both Mdr1a- and PXR-GFP knockin rats, with 50% of the F1 progeny corresponding to heterozygous mutants. Similar work was performed to target the *ROSA26* locus to integrate a GFP fragment, and the efficiency reported was 2% (Hermann *et al.* 2012).

Although the donor vectors used in *in vivo* genome editing contain relatively short homology arms for the targeted integration of SNVs that require only a few nucleotide substitutions, their construction is still a disproportionately laborious and time-consuming task. The use of synthetic single stranded DNA oligonucleotides (ssOligos) as donors for HDR can bypass this process. Davis and colleagues reported ZFN-mediated targeted integration of point mutations with ssOligos in several human cell lines with efficiencies that were up to twice those achieved using conventional targeting vectors (Chen *et al.* 2011). Kühn and colleagues applied ssOligo donor to produce knockin mice carrying SNVs (Meyer *et al.* 2012). They first generated a knockin mouse carrying a G19V missense and several silent SNVs in the *Rab38* gene, which encodes a small GTPase whose mutation results in a brown coat color, by co-injecting ZFNs with a conventional targeting vector. The targeting efficiency was 3.5% (three of 87 newborns), which is comparable to the efficiency they reported in their pioneering work (Meyer *et al.* 2010). All three founders exhibited efficient germline transmission, resulting in a brown coat color in F2 homozygous mutants (Meyer *et al.* 2012). Next, they co-injected the same ZFNs with a 144 nucleotide (nt) ssOligo containing seven substitutions into one-cell mouse embryos. They obtained one partially targeted mutant from 60 newborns with an efficiency of 1.7%, and the mutation was successfully transmitted to the F1 progeny. This work clearly reveals the enormous potential that ssOligos have for the replacement of conventional gene-targeting vectors in *in vivo* genome editing, which should greatly facilitate the rapid production of knockin mice.

In early 2013, Kühn and colleagues also generated *Rab38* G19V knockin mice by TALENs using an ssOligo (Wefers *et al.* 2013). They first constructed TALENs targeting the same region of the *Rab38* gene previously targeted by ZFNs, and found that the activity of the TALEN system was approximately twice that of ZFNs. Next, they co-injected TALENs and a ssOligo into one-cell mouse embryos and obtained one founder mouse carrying a partially targeted G19V allele from 117 newborns (an efficiency of 0.9%). The G19V allele was successfully transmitted to the F1 progeny. They also co-injected TALENs with a conventional targeting vector, rather than the ssOligo, and obtained one knockin founder carrying the G19V allele from 50 newborns (efficiency 2%). The G19V allele was also successfully transmitted to F1 progeny. As the construction of TALENs is much simpler than that of ZFNs, rapid production of knockin mice can be achieved using a combination of TALENs and ssOligos. However, the relatively low knockin efficiency of TALENs is a bottleneck that limits the dissemination of the method. To expand the applicability of TALEN-mediated *in vivo* genome editing, we developed highly active TALENs in collaboration with Dr Yamamoto's group at Hiroshima University. We focused on glutamate transporters, which are essential molecules that keep extracellular glutamate concentrations below neurotoxic levels (Tanaka *et al.* 1997; Watase *et al.* 1998; Matsugami *et al.* 2006; Aida *et al.* 2012). We previously reported *GLAST*, a glial glutamate transporter, knockout mouse as the first model for normal tension glaucoma (Harada *et al.* 1998, 2007; Bai *et al.* 2013a,b; Namekata *et al.* 2013). We also recently discovered deleterious missense mutations in *EAAT1*, a human orthologue of *GLAST*, in patients with glaucoma (Yanagisawa *et al.* unpubl. data, 2013). To

generate knockin mice carrying these SNVs in the *GLAST* gene, we co-injected highly active TALENs targeting *GLAST* into one-cell mouse embryos with ssOligos carrying each SNV. We obtained several germline-competent knockin founders with targeting efficiency of approximately 20% (Aida *et al.* unpubl. data, 2013). This study yielded the highest reported efficiency, which was almost 25-fold higher than the efficiency in a previous report by Wefers *et al.* As a single microinjection is sufficient to obtain several knockin founders, our TALEN technology provides a fast and efficient approach for the production of genetic mouse models that reproduce the disease-associated SNVs of complex diseases. Recently, Kühn and colleagues reported improved knockin efficiencies that were up to 8%, using TALEN mRNAs transcribed from plasmids containing a poly A tail (Panda *et al.* 2013).

Later, Jaenisch and colleagues reported the groundbreaking production of mice carrying multiple knockin alleles in different genes using CRISPR/Cas-mediated *in vivo* genome editing with extremely high efficiency (Wang *et al.* 2013a). They co-injected fertilized eggs with Cas9 mRNA, *Tet1* and *Tet2* guide RNAs, and 126 nt ssOligos to substitute a SacI site in *Tet1* and an EcoRV site in *Tet2* with EcoRI sites. Surprisingly, the vast majority (70–80%) of newborns carried EcoRI sites at *Tet1* or *Tet2* loci and some were homozygous for the EcoRI sites. Further, 60% of the newborns had EcoRI sites at both *Tet1* and *Tet2* loci.

Soon after this major accomplishment, Jaenisch and colleagues also produced knockin mice carrying longer DNA insertions by CRISPR/Cas-mediated *in vivo* genome editing (Yang *et al.* 2013). They first targeted the last codon of the *Sox2* gene with an ssOligo containing 42 nt short V5 epitope tag, and obtained targeted embryos and newborns with 34% efficiency. Next, they targeted the last codon of the *Nanog* gene with larger plasmid vector containing p2A-mCherry reporter cassette, and obtained targeted embryos and newborns with 8% efficiency. Further, they targeted the 3′ end of the *Oct4* gene with a plasmid vector containing 3 kb sequence of IRES-EGFP-loxP-Neo-loxP reporter cassette, and obtained targeted newborns with an efficiency of 30%. Finally, they also successfully generated knockin mice carrying a conditional allele of *Mecp2*, by simultaneously targeting with two loxP-containing ssOligos, and obtained targeted embryos and newborns carrying two loxP sites in one allele with an efficiency of 16%. Thus, knockin mice carrying, not only a SNV, but also longer DNA fragments, can now be created within a month using *in vivo* genome editing with high efficiency (Fig. 2). Taken together, almost everything achieved by ES cell-based gene targeting can now be performed by the *in vivo* genome editing technologies. Further, the new techniques allow previously impossible achievements, such as ultra-rapid production, biallelic targeting in F0 mice and multiplexing, leading genome editing to be the method of first choice for gene targeting.

Off-target effects

The off-target effect, which involves non-specific recognition and digestion at non-targeted regions by ZFNs, TALENs, and the CRISPR/Cas system, has been extensively discussed in the field of genome editing. When compared to ZFNs, TALENs produce only minimal off-target effects (less than a tenth), even at highly similar non-specific target sites with only two mismatches in the TALEN recognition sequence in human cells (Mussolino *et al.* 2011). Consistent with *in vitro* data, three papers describing TALEN-mediated *in vivo* genome editing in mice reported no off-target effects at a total of 15 potential off-target sites, containing only one mismatch, for four TALEN pairs (Panda *et al.* 2013; Qiu *et al.* 2013; Sung *et al.* 2013). Thus, in addition to basic research, TALENs may be applicable to therapeutics, a field that demands high-specificity.

Although the CRISPR/Cas system is an easy, quick, and highly efficient genome editing tool, the small size of the sequence (20 nt) required for DNA-RNA hybridization may make off-target effects more frequent with the CRISPR/Cas system than with TALENs or ZFNs. Recent large-scale systematic reports revealed an unexpectedly high frequency off-target effects using the CRISPR/Cas system in several human cell lines (Fu *et al.* 2013; Hsu *et al.* 2013; Pattanayak *et al.* 2013). According to these reports, the CRISPR/Cas system can cleave off-target sites containing even up to five mismatches (Fu *et al.* 2013). Jaenisch and colleagues investigated potential off-target sites using their knockout and knockin mice, as well as newly established mouse ES cells, to examine the specificity of the CRISPR/Cas system *in vivo* (Wang *et al.* 2013a; Yang *et al.* 2013). Through analyses of 54 potential off-target sites for seven guide RNAs, they found several non-specific digestions at three sites containing one or two mismatches. These results indicate that off-target effects in the CRISPR/Cas system do exist *in vivo*, but may be lower than predicted from *in vitro* studies using human cell lines.

As the majority of recent studies have focused on selected candidates for potential off-target effects, unbiased and genome-wide characterization of off-target sites through whole-genome sequencing will be required to guide the more sophisticated and specific design of RNAs.

To reduce non-specific off-target effects in the CRISPR/Cas system, Cas9 nickase, a mutant form of Cas9 that cleaves single stranded DNA, may provide an alternative for the induction of HDR (Cong *et al.* 2013; Mali *et al.* 2013). Zhang and colleagues recently reported that off-target effects could be reduced by using nickase and a pair of guide RNAs, without affecting on-target cleavage activity (Ran *et al.* 2013). They also revealed that this double-nicking strategy could efficiently cleave on-target sites in mouse zygotes. In combination with future developments using mutant Cas9 variants or other more specific Cas9 orthologues, these methods could reduce off-target effects in the CRISPR/Cas system.

The impact of *in vivo* genome editing

In Figure 2, we summarize the time course for the production of gene-targeted mice by conventional ES cell-based methods and *in vivo* genome editing by ZFNs, TALENs, and the CRISPR/Cas system. At best, it takes approximately 1 year to obtain a homozygous mutant by the conventional ES cell-based method. Also, it is common to spend a year or more obtaining germline competent chimeric founders. However, *in vivo* genome editing is revolutionizing these complex processes and enables ultra-rapid production of gene-targeted mice. In many cases, a genetically mosaic F0 founder and F2 homozygous knockout or knockin mouse can be obtained within a month and approximately 7 months, respectively. Further, in the best cases, as reported by several groups (Meyer *et al.* 2010; Hermann *et al.* 2012; Qiu *et al.* 2013; Sung *et al.* 2013; Wang *et al.* 2013a; Wu *et al.* 2013), biallelically targeted homozygous knockout or knockin mice can be obtained within a month. Thus, the genome editing revolution provides practical and exciting opportunities for the research community to freely and rapidly generate gene-targeted mice.

We now have the means to functionally investigate the consequences of millions of rare SNVs *in vivo* using "humanized" mice carrying equivalent variants. The cutting-edge work of Gleeson and colleagues demonstrated an interdisciplinary, sequencing era approach that integrates human genetics and mouse models (Novarino *et al.* 2012). They performed exome sequencing in consanguineous families with ASD, epilepsy, and intellectual disability and identified homozygous gene-disrupting SNVs in the *BCKDK* gene, which inactivates an enzyme complex essential for the catabolism of branched-chain amino acids (BCAAs). Because the SNVs resulted in disruption of the BCKDK gene, instead of generating knockin mice carrying the SNVs, they were able to investigate BCKDK knockout mice that showed reduced BCAAs in various tissues and neurological abnormalities, similar to other mouse models for ASD. In addition to BCAAs, they discovered imbalanced amino acid levels in the mutant brain that may contribute to the defects in neurotransmitter synthesis and subsequent neurological abnormalities. Finally, they tried to treat the mutant mice and patients using dietary supplementation with BCAAs and successfully reversed neurological abnormalities in the mutant mice and normalized plasma BCAA levels in patients (Novarino *et al.* 2012). Because the vast majority of rare SNVs are missense or synonymous, instead of gene-disrupting nonsense, splice site, or frameshift variants (Veltman & Brunner 2012), the production of knockin mouse models carrying such variants will be essential. Thus, *in vivo* genome editing drastically accelerates functional investigation of rare SNVs.

In vivo genome editing also accelerates functional research of common SNVs in intronic or intergenic regions indicated by the ENCODE (Encyclopedia of DNA Elements) project or GWAS studies (ENCODE Project Consortium *et al.* 2012; Maurano *et al.* 2012), in addition to those in protein-coding sequences. Cutting-edge work by Taipale and colleagues demonstrated the utility of gene-targeted mouse models in investigating the function of a GWAS-identified SNV (Sur *et al.* 2012). They focused on a conserved 500 kb region upstream of the *MYC* oncogene, where multiple cancer-associated SNVs have been mapped. They generated mutant mice lacking the region containing the SNV strongly associated with cancer, and found that the mutant mice were resistant to tumorigenesis (Sur *et al.* 2012). Further, Sabeti and colleagues used precisely modified knockin mice carrying a V370A SNV in the ectodysplasin receptor, which resulted in the identification of GWAS as one of the strongest candidates for recent positive selection in human evolution (Kamberov *et al.* 2013). They found that the knockin mice not only recapitulated the human phenotype, but also had previously unknown traits which were, surprisingly, also confirmed in human. As most common SNVs identified by GWAS can only explain relatively small contributions to disease risk, and the functional interpretation of non-coding SNVs is difficult, the generation of knockin mice by the time-consuming, laborious, and expensive process of ES cell-based conventional gene targeting is now considered disproportionate. The advent of *in vivo* genome editing technology has transformed this situation, enabling the mouse as a useful animal model system for the functional analysis of common, non-coding SNVs.

Further, genome editing technologies allow previously impossible gene targeting in mice. First, the methods allow gene targeting at the locus where traditional homologous recombination cannot be applied, such as the Y chromosome. Because the Y chromosome has unique structure containing many palindromes, conventional gene targeting in ES cells has failed. Jaenisch and colleagues targeted *Sry* and *Uty* genes on Y chromosome in mouse ES cells by using TALENs, and successfully obtained knockout mice lacking *Sry* or *Uty* (Wang *et al.* 2013b). Thus, high sequence specificity of TALENs provides a novel approach for genetic manipulation of the Y chromosome. Second, the methods allow double gene targeting at the neighboring loci. When two genes are located next to each other on the same chromosome, it is almost impossible to obtain double knockout mice by crossing two single knockout mice. Thus, the researchers have generated double-targeted ES cells by sequential targeting, a process much more time-consuming, laborious, and expensive than single gene targeting (Kitajima *et al.* 2000). As Jaenisch and colleagues demonstrated (Wang *et al.* 2013a), now, multiple genes can be targeted simultaneously by *in vivo* genome editing, thus providing opportunities to investigate cooperative roles of functionally redundant, clustered genes. Third, the methods allow gene targeting in diverse genetic backgrounds of mouse strains. In traditional gene targeting, ES cells derived from 129 mouse strain are most often used due to high efficiency of gene targeting. However, it is preferred to perform subsequent analyses of targeted mice on C57BL/6 genetic background. Thus, time-consuming backcrossing which takes at least 1 year is essential. As several groups demonstrated (Davies *et al.* 2013; Qiu *et al.* 2013), *in vivo* genome editing can be applicable to any mouse strain and provide opportunities to analyze the targeted mice immediately without backcrossing.

Overall, *in vivo* genome editing technology drastically accelerates the translation of human genetics into the mouse, in addition to other higher species such as primates (Sasaki *et al.* 2009), and should revolutionize our understanding of the functional consequences of human genomic diversity in health and disease.

Acknowledgments

This work was supported by Strategic Research Program for Brain Sciences (SRPBS) from Ministry of Education, Culture, Sports, Science and Technology of Japan, and CREST from Japan Science Technology Agency to K.T. We thank T. Yamamoto and T. Sakuma (Hiroshima University) for technical support and useful discussions, H. Ishikubo and T. Usami (Tokyo Medical and Dental University) for technical support, and M. Abe (Niigata University) and K. Tanaka (Keio University) for useful discussions.

References

1000 Genomes Project Consortium, Abecasis, G. R., Auton, A., Brooks, L. D., DePristo, M. A., Durbin, R. M., Handsaker, R. E., Kang, H. M., Marth, G. T. & McVean, G. A. 2012. An integrated map of genetic variation from 1,092 human genomes. *Nature* **491**, 56–65.

Aida, T., Ito, Y., Takahashi, Y. K. & Tanaka, K. 2012. Overstimulation of NMDA receptors impairs early brain development *in vivo*. *PLoS ONE* **7**, e36853.

Bai, N., Hayashi, H., Aida, T., Namekata, K., Harada, T., Mishina, M. & Tanaka, K. 2013a. Dock3 interaction with a glutamate-receptor NR2D subunit protects neurons from excitotoxicity. *Mol. Brain* **6**, 22.

Bai, N., Aida, T., Yanagisawa, M., Katou, S., Sakimura, K., Mishina, M. & Tanaka, K. 2013b. NMDA receptor subunits have different roles in NMDA-induced neurotoxicity in the retina. *Mol. Brain* **6**, 34.

Capecchi, M. R. 2005. Gene targeting in mice: functional analysis of the mammalian genome for the twenty-first century. *Nat. Rev. Genet.* **6**, 507–512.

Carbery, I. D., Ji, D., Harrington, A., Brown, V., Weinstein, E. J., Liaw, L. & Cui, X. 2010. Targeted genome modification in mice using zinc-finger nucleases. *Genetics* **186**, 451–459.

Chen, F., Pruett-Miller, S. M., Huang, Y., Gjoka, M., Duda, K., Taunton, J., Collingwood, T. N., Frodin, M. & Davis, G. D. 2011. High-frequency genome editing using ssDNA oligonucleotides with zinc-finger nucleases. *Nat. Methods* **8**, 753–755.

Cirulli, E. T. & Goldstein, D. B. 2010. Uncovering the roles of rare variants in common disease through whole-genome sequencing. *Nat. Rev. Genet.* **11**, 415–425.

Cohen, S., Gabel, H. W., Hemberg, M., Hutchinson, A. N., Sadacca, L. A., Ebert, D. H., Harmin, D. A., Greenberg, R. S., Verdine, V. K., Zhou, Z., Wetsel, W. C., West, A. E. & Greenberg, M. E. 2011. Genome-wide activity-dependent MeCP2 phosphorylation regulates nervous system development and function. *Neuron* **72**, 72–85.

Cong, L., Ran, F. A., Cox, D., Lin, S., Barretto, R., Habib, N., Hsu, P. D., Wu, X., Jiang, W., Marraffini, L. A. & Zhang, F. 2013. Multiplex genome engineering using CRISPR/Cas systems. *Science* **339**, 819–823.

Cui, X., Ji, D., Fisher, D. A., Wu, Y., Briner, D. M. & Weinstein, E. J. 2011. Targeted integration in rat and mouse embryos with zinc-finger nucleases. *Nat. Biotechnol.* **29**, 64–67.

Davies, B., Davies, G., Preece, C., Puliyadi, R., Szumska, D. & Bhattacharya, S. 2013. Site specific mutation of the Zic2 locus by microinjection of TALEN mRNA in mouse CD1, C3H and C57BL/6J oocytes. *PLoS ONE* **8**, e60216.

Ebert, D. H., Gabel, H. W., Robinson, N. D., Kastan, N. R., Hu, L. S., Cohen, S., Navarro, A. J., Lyst, M. J., Ekiert, R., Bird, A. P. & Greenberg, M. E. 2013. Activity-dependent phosphorylation of MeCP2 threonine 308 regulates interaction with NCoR. *Nature* **499**, 341–345.

ENCODE Project Consortium, Bernstein, B. E., Birney, E., Dunham, I., Green, E. D., Gunter, C. & Snyder, M. 2012. An integrated encyclopedia of DNA elements in the human genome. *Nature* **489**, 57–74.

Fu, Y., Foden, J. A., Khayter, C., Maeder, M. L., Reyon, D., Joung, J. K. & Sander, J. D. 2013. High-frequency off-target mutagenesis induced by CRISPR-Cas nucleases in human cells. *Nat. Biotechnol.* **31**, 822–826.

Geurts, A. M., Cost, G. J., Freyvert, Y., Zeitler, B., Miller, J. C., Choi, V. M., Jenkins, S. S., Wood, A., Cui, X., Meng, X., Vincent, A., Lam, S., Michalkiewicz, M., Schilling, R., Foeckler, J., Kalloway, S., Weiler, H., Ménoret, S., Anegon, I., Davis, G. D., Zhang, L., Rebar, E. J., Gregory, P. D., Urnov, F. D., Jacob, H. J. & Buelow, R. 2009. Knockout rats via embryo microinjection of zinc-finger nucleases. *Science* **325**, 433.

Goffin, D., Allen, M., Zhang, L., Amorim, M., Wang, I. T., Reyes, A. R., Mercado-Berton, A., Ong, C., Cohen, S., Hu, L., Blendy, J. A., Carlson, G. C., Siegel, S. J., Greenberg, M. E. & Zhou, Z. 2011. Rett syndrome mutation MeCP2 T158A disrupts DNA binding, protein stability and ERP responses. *Nat. Neurosci.* **15**, 274–283.

Harada, T., Harada, C., Watanabe, M., Inoue, Y., Sakagawa, T., Nakayama, N., Sasaki, S., Okuyama, S., Watase, K., Wada, K. & Tanaka, K. 1998. Functions of the two glutamate transporters GLAST and GLT-1 in the retina. *Proc. Natl Acad. Sci. USA* **95**, 4663–4666.

Harada, T., Harada, C., Nakamura, K., Quah, H. M., Okumura, A., Namekata, K., Saeki, T., Aihara, M., Yoshida, H., Mitani, A. & Tanaka, K. 2007. The potential role of glutamate transporters in the pathogenesis of normal tension glaucoma. *J. Clin. Invest.* **117**, 1763–1770.

Hermann, M., Maeder, M. L., Rector, K., Ruiz, J., Becher, B., Bürki, K., Khayter, C., Aguzzi, A., Joung, J. K., Buch, T. & Pelczar, P. 2012. Evaluation of OPEN zinc finger nucleases for direct gene targeting of the ROSA26 locus in mouse embryos. *PLoS ONE* **7**, e41796.

Hsu, P. D., Scott, D. A., Weinstein, J. A., Ran, F. A., Konermann, S., Agarwala, V., Li, Y., Fine, E. J., Wu, X., Shalem, O., Cradick, T. J., Marraffini, L. A., Bao, G. & Zhang, F. 2013. DNA targeting specificity of RNA-guided Cas9 nucleases. *Nat. Biotechnol.* **31**, 827–832.

Iossifov, I., Ronemus, M., Levy, D., Wang, Z., Hakker, I., Rosenbaum, J., Yamrom, B., Lee, Y. H., Narzisi, G., Leotta, A., Kendall, J., Grabowska, E., Ma, B., Marks1, S., Rodgers, L., Stepansky, A., Troge, J., Andrews, P., Bekritsky, M., Pradhan, K., Ghiban, E., Kramer, M., Parla, J., Demeter, R., Fulton, L. L., Fulton, R. S., Magrini, V. J., Ye, K., Darnell, J. C., Darnell, R. B., Mardis, E. R., Wilson, R. K., Schatz, M. C., McCombie, W. R. & Wigler, M. 2012. De novo gene disruptions in children on the autistic spectrum. *Neuron* **74**, 285–299.

Jentarra, G. M., Olfers, S. L., Rice, S. G., Srivastava, N., Homanics, G. E., Blue, M., Naidu, S. & Narayanan, V. 2010. Abnormalities of cell packing density and dendritic complexity in the MeCP2 A140V mouse model of Rett syndrome/X-linked mental retardation. *BMC Neurosci.* **11**, 19.

Joung, J. K. & Sander, J. D. 2013. TALENs: a widely applicable technology for targeted genome editing. *Nat. Rev. Mol. Cell Biol.* **14**, 49–55.

Kamberov, Y. G., Wang, S., Tan, J., Gerbault, P., Wark, A., Tan, L., Yang, Y., Li, S., Tang, K., Chen, H., Powell, A., Itan, Y., Fuller, D., Lohmueller, J., Mao, J., Schachar, A., Paymer, M., Hostetter, E., Byrne, E., Burnett, M., McMahon, A. P., Thomas, M. G., Lieberman, D. E., Jin, L., Tabin, C. J., Morgan, B. A. & Sabeti, P. C. 2013. Modeling recent human evolution in mice by expression of a selected EDAR variant. *Cell* **152**, 691–702.

Kitajima, S., Takagi, A., Inoue, T. & Saga, Y. 2000. MesP1 and MesP2 are essential for the development of cardiac mesoderm. *Development* **127**, 3215–3226.

Li, D., Qiu, Z., Shao, Y., Chen, Y., Guan, Y., Liu, M., Li, Y., Gao, N., Wang, L., Lu, X., Zhao, Y. & Liu, M. 2013. Heritable gene targeting in the mouse and rat using a CRISPR-Cas system. *Nat. Biotechnol.* **31**, 681–683.

Lyst, M. J., Ekiert, R., Ebert, D. H., Merusi, C., Nowak, J., Selfridge, J., Guy, J., Kastan, N. R., Robinson, N. D., de Lima Alves, F., Rappsilber, J., Greenberg, M. E. & Bird, A. 2013. Rett syndrome mutations abolish the interaction of MeCP2 with the NCoR/SMRT co-repressor. *Nat. Neurosci.* **16**, 898–902.

Mali, P., Yang, L., Esvelt, K. M., Aach, J., Guell, M., DiCarlo, J. E., Norville, J. E. & Church, G. M. 2013. RNA-guided human genome engineering via Cas9. *Science* **339**, 823–826.

Manolio, T. A., Collins, F. S., Cox, N. J., Goldstein, D. B., Hindorff, L. A., Hunter, D. J., McCarthy, M. I., Ramos, E. M., Cardon, L. R., Chakravarti, A., Cho, J. H., Guttmacher, A. E., Kong, A., Kruglyak, L., Mardis, E., Rotimi, C. N., Slatkin, M., Valle, D., Whittemore, A. S., Boehnke, M., Clark, A. G., Eichler, E. E., Gibson, G., Haines, J. L., Mackay, T. F., McCarroll, S. A. & Visscher, P. M. 2009. Finding the missing heritability of complex diseases. *Nature* **461**, 747–753.

Matsugami, T. R., Tanemura, K., Mieda, M., Nakatomi, R., Yamada, K., Kondo, T., Ogawa, M., Obata, K., Watanabe, M., Hashikawa, T. & Tanaka, K. 2006. Indispensability of the glutamate transporters GLAST and GLT1 to brain development. *Proc. Natl Acad. Sci. USA* **103**, 12161–12166.

Maurano, M. T., Humbert, R., Rynes, E., Thurman, R. E., Haugen, E., Wang, H., Reynolds, A. P., Sandstrom, R., Qu, H., Brody, J., Shafer, A., Neri, F., Lee, K., Kutyavin, T., Stehling-Sun, S., Johnson, A. K., Canfield, T. K., Giste, E., Diegel, M., Bates, D., Hansen, R. S., Neph, S., Sabo, P. J., Heimfeld, S., Raubitschek, A., Ziegler, S., Cotsapas, C., Sotoodehnia, N., Glass, I., Sunyaev, S. R., Kaul, R. & Stamatoyannopoulos, J. A. 2012. Systematic localization of common disease-associated variation in regulatory DNA. *Science* **337**, 1190–1195.

Menke, D. B. 2013. Engineering subtle targeted mutations into the mouse genome. *Genesis* **51**, 605–618.

Meyer, M., de Angelis, M. H., Wurst, W. & Kuhn, R. 2010. Gene targeting by homologous recombination in mouse zygotes mediated by zinc-finger nucleases. *Proc. Natl Acad. Sci. USA* **107**, 15022–15026.

Meyer, M., Ortiz, O., Hrabe de Angelis, M., Wurst, W. & Kuhn, R. 2012. Modeling disease mutations by gene targeting in one-cell mouse embryos. *Proc. Natl Acad. Sci. USA* **109**, 9354–9359.

Mussolino, C., Morbitzer, R., Lütge, F., Dannemann, N., Lahaye, T. & Cathomen, T. 2011. A novel TALE nuclease scaffold enables high genome editing activity in combination with low toxicity. *Nucleic Acids Res.* **39**, 9283–9293.

Namekata, K., Kimura, A., Kawamura, K., Guo, X., Harada, C., Tanaka, K. & Harada, T. 2013. Dock3 attenuates neural cell death due to NMDA neurotoxicity and oxidative stress in a mouse model of normal tension glaucoma. *Cell Death Differ.* **20**, 1250–1256.

Neale, B. M., Kou, Y., Liu, L., Ma'ayan, A., Samocha, K. E., Sabo, A., Lin, C. F., Stevens, C., Wang, L. S., Makarov, V., Polak, P., Yoon, S., Maguire, J., Crawford, E. L., Campbell, N. G., Geller, E. T., Valladares, O., Schafer, C., Liu, H., Zhao, T., Cai, G., Lihm, J., Dannenfelser, R., Jabado, O., Peralta, Z., Nagaswamy, U., Muzny, D., Reid, J. G.,

Newsham, I., Wu, Y., Lewis, L., Han, Y., Voight, B. F., Lim, E., Rossin, E., Kirby, A., Flannick, J., Fromer, M., Shakir, K., Fennell, T., Garimella, K., Banks, E., Poplin, R., Gabriel, S., DePristo, M., Wimbish, J. R., Boone, B. E., Levy, S. E., Betancur, C., Sunyaev, S., Boerwinkle, E., Buxbaum, J. D., Cook, E. H., Devlin, B., Gibbs, R. A., Roeder, K., Schellenberg, G. D., Sutcliffe, J. S. & Daly, M. J. 2012. Patterns and rates of exonic de novo mutations in autism spectrum disorders. *Nature* **485**, 242–245.

Novarino, G., El-Fishawy, P., Kayserili, H., Meguid, N. A., Scott, E. M., Schroth, J., Silhavy, J. L., Kara, M., Khalil, R. O., Ben-Omran, T., Ercan-Sencicek, A. G., Hashish, A. F., Sanders, S. J., Gupta, A. R., Hashem, H. S., Matern, D., Gabriel, S., Sweetman, L., Rahimi, Y., Harris, R. A., State, M. W. & Gleeson, J. G. 2012. Mutations in BCKD-kinase lead to a potentially treatable form of autism with epilepsy. *Science* **338**, 394–397.

O'Roak, B. J., Vives, L., Girirajan, S., Karakoc, E., Krumm, N., Coe, B. P., Levy, R., Ko, A., Lee, C., Smith, J. D., Turner, E. H., Stanaway, I. B., Vernot, B., Malig, M., Baker, C., Reilly, B., Akey, J. M., Borenstein, E., Rieder, M. J., Nickerson, D. A., Bernier, R., Shendure, J. & Eichler, E. E.. 2012. Sporadic autism exomes reveal a highly interconnected protein network of de novo mutations. *Nature* **485**, 246–250.

Panda, S. K., Wefers, B., Ortiz, O., Floss, T., Schmid, B., Haass, C., Wurst, W. & Kühn, R. 2013. Highly efficient targeted mutagenesis in mice using TALENs. *Genetics* doi: 10.1534/genetics.113.156570.

Pattanayak, V., Lin, S., Guilinger, J. P., Ma, E., Doudna, J. A. & Liu, D. R. 2013. High-throughput profiling of off-target DNA cleavage reveals RNA-programmed Cas9 nuclease specificity. *Nat. Biotechnol.* **31**, 839–843.

Qiu, Z., Liu, M., Chen, Z., Shao, Y., Pan, H., Wei, G., Yu, C., Zhang, L., Li, X., Wang, P., Fan, H. Y., Du, B., Liu, B. & Li, D. 2013. High-efficiency and heritable gene targeting in mouse by transcription activator-like effector nucleases. *Nucleic Acids Res.* **41**, e120.

Ran, F. A., Hsu, P. D., Lin, C. Y., Gootenberg, J. S., Konermann, S., Trevino, A. E., Scott, D. A., Inoue, A., Matoba, S., Zhang, Y. & Zhang, F. 2013. Double nicking by RNA-guided CRISPR Cas9 for enhanced genome editing specificity. *Cell* **154**, 1380–1389.

Raychaudhuri, S. 2011. Mapping rare and common causal alleles for complex human diseases. *Cell* **147**, 57–69.

Sanders, S. J., Murtha, M. T., Gupta, A. R., Murdoch, J. D., Raubeson, M. J., Willsey, A. J., Ercan-Sencicek, A. G., DiLullo, N. M., Parikshak, N. N., Stein, J. L., Walker, M. F., Ober, G. T., Teran, N. A., Song, Y., El-Fishawy, P., Murtha, R. C., Choi, M., Overton, J. D., Bjornson, R. D., Carriero, N. J., Meyer, K. A., Bilguvar, K., Mane, S. M., Sestan, N., Lifton, R. P., Günel, M., Roeder, K., Geschwind, D. H., Devlin, B. & State, M. W. 2012. De novo mutations revealed by whole-exome sequencing are strongly associated with autism. *Nature* **485**, 237–241.

Sasaki, E., Suemizu, H., Shimada, A., Hanazawa, K., Oiwa, R., Kamioka, M., Tomioka, I., Sotomaru, Y., Hirakawa, R., Eto, T., Shiozawa, S., Maeda, T., Ito, M., Ito, R., Kito, C., Yagihashi, C., Kawai, K., Miyoshi, H., Tanioka, Y., Tamaoki, N., Habu, S., Okano, H. & Nomura, T. 2009. Generation of transgenic non-human primates with germline transmission. *Nature* **459**, 523–527.

Shen, B., Zhang, J., Wu, H., Wang, J., Ma, K., Li, Z., Zhang, X., Zhang, P. & Huang, X. 2013. Generation of gene-modified mice via Cas9/RNA-mediated gene targeting. *Cell Res.* **23**, 720–723.

Skarnes, W. C., Rosen, B., West, A. P., Koutsourakis, M., Bushell, W., Iyer, V., Mujica, A. O., Thomas, M., Harrow, J., Cox, T., Jackson, D., Severin, J., Biggs, P., Fu, J., Nefedov, M., de Jong, P. J., Stewart, A. F. & Bradley, A. 2011. A conditional knockout resource for the genome-wide study of mouse gene function. *Nature* **474**, 337–342.

Sung, Y. H., Baek, I. J., Seong, J. K., Kim, J. S. & Lee, H. W. 2012. Mouse genetics: catalogue and scissors. *BMB Rep.* **45**, 686–692.

Sung, Y. H., Baek, I. J., Kim, D. H., Jeon, J., Lee, J., Lee, K., Jeong, D., Kim, J. S. & Lee, H. W. 2013. Knockout mice created by TALEN-mediated gene targeting. *Nat. Biotechnol.* **31**, 23–24.

Sur, I. K., Hallikas, O., Vähärautio, A., Yan, J., Turunen, M., Enge, M., Taipale, M., Karhu, A., Aaltonen, L. A. & Taipale, J. 2012. Mice lacking a Myc enhancer that includes human SNP rs6983267 are resistant to intestinal tumors. *Science* **338**, 1360–1363.

Tabuchi, K., Blundell, J., Etherton, M. R., Hammer, R. E., Liu, X., Powell, C. M. & Südhof, T. C. 2007. A neuroligin-3 mutation implicated in autism increases inhibitory synaptic transmission in mice. *Science* **318**, 71–76.

Tanaka, K., Watase, K., Manabe, T., Yamada, K., Watanabe, M., Takahashi, K., Iwama, H., Nishikawa, T., Ichihara, N., Kikuchi, T., Okuyama, S., Kawashima, N., Hori, S., Takimoto, M. & Wada, K. 1997. Epilepsy and exacerbation of brain injury in mice lacking the glutamate transporter GLT-1. *Science* **276**, 1699–1702.

Tao, J., Hu, K., Chang, Q., Wu, H., Sherman, N. E., Martinowich, K., Klose, R. J., Schanen, C., Jaenisch, R., Wang, W. & Sun, Y. E. 2009. Phosphorylation of MeCP2 at Serine 80 regulates its chromatin association and neurological function. *Proc. Natl Acad. Sci. USA* **106**, 4882–4887.

Urnov, F. D., Rebar, E. J., Holmes, M. C., Zhang, H. S. & Gregory, P. D. 2010. Genome editing with engineered zinc finger nucleases. *Nat. Rev. Genet.* **11**, 636–646.

Veltman, J. A. & Brunner, H. G. 2012. De novo mutations in human genetic disease. *Nat. Rev. Genet.* **13**, 565–575.

Wang, H., Yang, H., Shivalila, C. S., Dawlaty, M. M., Cheng, A. W., Zhang, F. & Jaenisch, R. 2013a. One-step generation of mice carrying mutations in multiple genes by CRISPR/Cas-mediated genome engineering. *Cell* **153**, 910–918.

Wang, H., Hu, Y. C., Markoulaki, S., Welstead, G. G., Cheng, A. W., Shivalila, C. S., Pyntikova, T., Dadon, D. B., Voytas, D. F., Bogdanove, A. J., Page, D. C. & Jaenisch, R. 2013b. TALEN-mediated editing of the mouse Y chromosome. *Nat. Biotechnol.* **31**, 530–532.

Watase, K., Hashimoto, K., Kano, M., Yamada, K., Watanabe, M., Inoue, Y., Okuyama, S., Sakagawa, T., Ogawa, S., Kawashima, N., Hori, S., Takimoto, M., Wada, K. & Tanaka, K. 1998. Motor discoordination and increased susceptibility to cerebellar injury in GLAST mutant mice. *Eur. J. Neurosci.* **10**, 976–988.

Wefers, B., Meyer, M., Ortiz, O., Hrabé de Angelis, M., Hansen, J., Wurst, W. & Kühn, R. 2013. Direct production of mouse disease models by embryo microinjection of TALENs and oligodeoxynucleotides. *Proc. Natl Acad. Sci. USA* **110**, 3782–3787.

White, J. K., Gerdin, A. K., Karp, N. A., Ryder, E., Buljan, M., Bussell, J. N., Salisbury, J., Clare, S., Ingham, N. J., Podrini, C., Houghton, R., Estabel, J., Bottomley, J. R., Melvin, D. G., Sunter, D., Adams, N. C., Tannahill, D., Logan, D. W.,

Macarthur, D. G., Flint, J., Mahajan, V. B., Tsang, S. H., Smyth, I., Watt, F. M., Skarnes, W. C., Dougan, G., Adams, D. J., Ramirez-Solis, R., Bradley, A. & Steel, K. P. & Sanger Institute Mouse Genetics Project. 2013. Genome-wide generation and systematic phenotyping of knockout mice reveals new roles for many genes. *Cell* **154**, 452–464.

Wu, J., Huang, Z., Ren, J., Zhang, Z., He, P., Li, Y., Ma, J., Chen, W., Zhang, Y., Zhou, X., Yang, Z., Wu, S. Q., Chen, L. & Han, J. 2013. Mlkl knockout mice demonstrate the indispensable role of Mlkl in necroptosis. *Cell Res.* **23**, 994–1006.

Yang, H., Wang, H., Shivalila, C. S., Cheng, A. W., Shi, L. & Jaenisch, R. 2013. One-Step generation of mice carrying reporter and conditional alleles by CRISPR/Cas-mediated genome engineering. *Cell* **154**, 1370–1379.

Acta Ophthalmologica

ACTA OPHTHALMOLOGICA 2013

Changes in visual acuity and intra-ocular pressure following bleb-related infection: the Japan Glaucoma Society Survey of Bleb-related Infection Report 2

Tetsuya Yamamoto,[1] Yasuaki Kuwayama,[2] Eiichi Nomura,[3] Hidenobu Tanihara[4] and Kazuhiko Mori[5] for the Study Group for the Japan Glaucoma Society Survey of Bleb-related Infection

[1]Department of Ophthalmology, Gifu University Graduate School of Medicine, Gifu, Japan
[2]Department of Ophthalmology, Osaka Koseinenkin Hospital, Osaka, Japan
[3]Department of Ophthalmology, Yokohama City University School of Medicine, Yokohama, Japan
[4]Department of Ophthalmology, Kumamoto University Graduate School of Medical Sciences, Kumamoto, Japan
[5]Department of Ophthalmology, Kyoto Prefectural University of Medicine, Kyoto, Japan

ABSTRACT.

Purpose: **To identify changes in visual acuity and intra-ocular pressure (IOP) 12 months after the development of bleb-related infection.**

Methods: **Data obtained from 146 eyes of 146 patients with bleb-related infection were analyzed as a part of the Japan Glaucoma Society Survey of Bleb-related Infection. Multiple logistic regression analysis was conducted to identify factors associated with poor prognosis in visual acuity and increased IOP and for being stage III.**

Results: **The logMAR increased by a mean of 0.140, 0.440, 1.099 and 1.122 at 12 months postinfection for stage I, II, IIIa and IIIb infections, respectively. The logMAR was significantly worse at 6 and 12 months postinfection in stage IIIb ($p = 0.002$ and $p = 0.003$, respectively; Wilcoxon signed-rank test) and at 6 months postinfection in stage IIIa ($p = 0.036$). The IOP was significantly elevated following infection in both stage IIIa and stage IIIb ($p = 0.028$ and $p = 0.008$ at 6 and 12 months, respectively, for stage IIIa; $p = 0.002$ and $p = 0.005$ for stage IIIb). The multiple logistic regression analysis revealed that being stage III and positive culture were significant risk factors for poor outcome for visual acuity (Odds ratio: 9.26 and 6.29, respectively) and that being stage III was a prognostic factor for increased IOP (Odds ratio: 8.33). Pseudophakia or aphakia was significantly associated with stage III and stage IIIb infections (Odds ratio: 2.85 and 6.30).**

Conclusions: **Stage III bleb-related infection causes significant visual loss and IOP elevation within 12 months after development. Therefore, preventative measures should be taken, especially in cases that are pseudophakic or aphakic.**

Key words: bleb-related infection – glaucoma – glaucoma surgery – intra-ocular pressure – trabeculectomy – visual acuity

Acta Ophthalmol. 2013: 91: e420–e426

doi: 10.1111/aos.12079

Introduction

Late-onset bleb-related ocular infection is a known, potentially blinding complication of glaucoma filtration surgery. (Katz et al. 1985; Mandelbaum et al. 1985; Greenfield et al. 1996; Kangas et al. 1997; Waheed et al. 1998; Song et al. 2002; Busbee et al. 2004; Leng et al. 2011; Rai et al. 2012). Although the reported incidence of bleb-related infection is highly variable (Mochizuki et al. 1997; Yamamoto et al. 2012), it is higher in cases of adjuvant antimetabolite use. Its incidence has been reported to be 1.5–13.8% in cases using intra-operative mitomycin C adjunctively, which were followed from 16 months to 8 years (Greenfield et al. 1996; Mochizuki et al. 1997; DeBry et al. 2002; Shigeeda et al. 2006; Sharan et al. 2009). Thus, this complication must be taken into consideration even before surgery is undertaken.

We have already reported on the clinical characteristics and microbial findings in bleb-related infection based on the Japan Glaucoma Society

Survey of Bleb-related Infection (JGSSBI), a 5-year-long, multicenter survey (Yamamoto et al. 2012). This survey compiled data on 170 bleb-related infections that developed in 156 patients involving 157 eyes. Among other findings, our analysis revealed that the period between the last glaucoma surgery and the development of infection was quite variable, lasting up to 41 years. Bleb leakage was noted significantly more frequently in eyes with repeated infection and Gram-positive bacteria were the major detected bacteria. In the present second report of the JGSSBI, we discuss the outcome of bleb-related infections in terms of visual acuity and intra-ocular pressure (IOP) 12 months after the development of a bleb-related infection.

Materials and Methods

The details of the JGSSBI are described elsewhere (Yamamoto et al. 2012). Briefly, this prospective study included a surveillance period of 5 years in which all patients with bleb-related infection were consecutively registered from 82 medical centres in Japan, and clinical and microbial data were collected. Institutional review board approval was obtained at each institution. In 36 clinics where there was no governing institutional review board, the Ethical Review Board of the Gifu University Hospital approved the study protocol for the clinics on the condition that the study would be conducted under the guidance of the University Hospital. All patients or their guardians gave written informed consent after thorough explanation of the study. The management of bleb-related infection was at the discretion of local investigators. Because cases from surgeries performed at ophthalmology clinics outside of the study centres were also included, pre-infection data collection might have been incomplete in some cases. Each infection was classified into one of three stages (Azuara-Branco & Katz 1998; Greenfield 1998): stage I denoted infections confined to the bleb site with a mild cell reaction in the anterior chamber; stage II denoted infections where the anterior chamber was the main locus and the vitreous was not involved; stage III denoted infections involving the vitreous. Stage III was subdivided into stages IIIa and IIIb (Yamamoto et al. 2011): stage IIIa denoted mild involvement to the vitreous and stage IIIb denoted more advanced involvement. The staging into category IIIa or IIIb was done mainly based on visibility of the fundus and vitreous opacity detected by B-mode echography.

A total of 170 infections developed in 157 eyes of 156 patients that were collected from 45 institutions. In the present study, only the cases where 6-month and/or 12-month follow-up results were available were analyzed. The following information was collected as postinfection data: use of glaucoma and other medication, postoperative complications, additional procedures or surgery, bleb appearance and results of ophthalmic examinations including visual acuity, refraction, IOP and visual field. Bleb appearance was determined according to a predetermined scoring system. The postinfection data were employed and analyzed if they were collected within 2 months of the designated period. In cases with multiple infections, we used data for the last infection.

Multiple logistic regression analysis was conducted to identify factors associated with poor prognosis in visual acuity and increased IOP. Poor visual prognosis was defined as an increase of logMAR of at least 0.5 units at 12 months following the development of bleb-related infection. Counting fingers was considered as 0.004, hand motion as 0.002, light sensation as 0.001 and no light sensation as 0.0004 for this calculation. Poor IOP prognosis was defined as IOP elevation of 5 mmHg or greater at 12 months. The following were considered to be potentially associated factors: age, gender, interval between surgery and development of infection, stage of the infection, detection of bacteria, detection of *Streptococcus* species, history of bleb leakage, type of conjunctival incision and pre-infection IOP. Stage factors were enrolled as nominal variables; for example, variable 'stage I' was able to take the value Yes which meant 'being stage I' or the value No meaning 'not being stage I' and so on. In addition, we conducted multiple logistic regression analysis to identify factors associated with being stage IIIa, stage IIIb or stage III, i.e. stage IIIa or stage IIIb. Candidates for associated factors were age, gender, interval between surgery and development of infection, lens status, detection of bacteria, detection of *Streptococcus* species, history of bleb leakage, type of conjunctival incision and pre-infection IOP.

Statistical analysis as well as logistic regression analysis was conducted via the SPSS 16.0 J software (SPSS Japan Inc., Tokyo, Japan) or the IBM SPSS Statistics software version 20.0 (IBM Japan Ltd., Tokyo, Japan). p-Values <0.05 were considered statistically significant.

Results

Six-month and 12-month follow-up data were available in 146 eyes of 146 patients. The 6-month data were available for 134 eyes and the 12-month data for 112 eyes. The backgrounds of the subjects were shown in Tables 1 and 2. All eyes were intensively treated with antibiotic therapy and surgery where indicated. In total, 45 eyes underwent vitreous surgery and four eyes required enucleation or evisceration of the eyeball. In addition, six eyes ended up with phthisis bulbi.

Visual acuity data were available for 113 eyes at 6 months postinfection and for 107 eyes at 12 months postinfection. Pairs of pre- and postinfection visual acuities were available for 96 eyes at 6 months postinfection and for 93 eyes at 12 months postinfection, respectively. A total of 10 eyes that were enucleated or eviscerated or had developed phthisis bulbi were included as having visual acuity described as no light sensation. Table 3 shows the pre and postinfection visual acuities and Figs 1–4 demonstrate the relationship between them in all cases where paired data were available. The postinfection logMAR was significantly deteriorated in all cases ($p = 0.000$ at both 6 and 12 months postinfection; Wilcoxon signed-rank test), in stage IIIb ($p = 0.002$ and $p = 0.003$ at 6 and 12 months postinfection, respectively) and in stage IIIa at 6 months postinfection ($p = 0.036$). It did not change in stages I and II, and at 12 months postinfection in stage IIIa. The logMAR increased by a mean of 0.140, 0.440, 1.099 and

Table 1. Patients' backgrounds.

Last glaucoma surgery	
Trabeculectomy	118 eyes
Trabeculectomy with PEA/IOL	19 eyes
Non-penetrating trabeculectomy	2 eyes
Trabeculectomy combined with IOL	1 eye
Scheie's thermal sclerostomy	3 eyes
Unknown	3 eyes
Sex	
Male	102 eyes
Female	44 eyes
Glaucoma subtype	
Primary open angle glaucoma	66 eyes
Normal tension glaucoma	8 eyes
Primary angle closure glaucoma	3 eyes
Developmental glaucoma	18 eyes
Secondary glaucoma	34 eyes
Use of antimetabolites	
Mitomycin C alone	116 eyes
Mitomycin C and 5-fluorouracil	2 eyes
5-Fluorouracil alone	1 eye
No antimetabolites	3 eyes
Unknown	24 eyes
Stage of bleb-related infection at diagnosis	
Stage I	73 eyes (50.0%)
Stage II	27 eyes (18.5%)
Stage IIIa	15 eyes (10.3%)
Stage IIIb	31 eyes (21.2%)
Bleb location	
Between the 10 to 2 o'clock positions	145 eyes
3 o'clock position	1 eye
Bleb leakage noticed before developing infection	
Yes	70 eyes (47.9%)
No	54 eyes (37.0%)
Unknown	22 eyes (15.1%)
IOP before infection (undetermined in four eyes)	
Mean ± standard deviation	10.0 ± 3.9 mmHg
Range	2–27 mmHg

PEA = phacoemulsification and aspiration, IOL = intra-ocular lens implantation, IOP = intra-ocular pressure.

Table 2. Result of bacterial cultures.

Culture done	128/146 (87.7%)
Culture positive	69/128 (53.9%)
Conjunctival scraping	90
Anterior chamber tapping	28
Vitreous tapping	25
Strains isolated	73
Staphylococcus aureus (MRSA included)	14
CNS (MRSE included)	14
Streptococcus spp.	24
Corynebacterium spp.	7
Enterococcus spp.	4
Haemophilus influenzae	4
Others	6

MRSA = methicillin-resistant *Staphylococcus aureus*, CNS = coagulase-negative *Staphylococcus*, MRSE = methicillin-resistant *Staphylococcus epidermidis*, spp species.

1.122 at 12 months postinfection for stage I, II, IIIa and IIIb infections, respectively. Table 4 shows the visual acuity at the last available visit after infection for cases in which preinfection visual acuity was at least 20/40.

Data on IOP were available for 123 eyes at 6 months postinfection and for 102 eyes at 12 months postinfection. Pairs of pre and postinfection IOPs were available for 119 eyes at 6 months and for 98 eyes at 12 months, respectively, following development of infection. The eyes that were enucleated or eviscerated or had developed phthisis bulbi were excluded from the IOP analysis at postinfection. Table 5 shows the preinfection and postinfection IOPs and Figs 5–8 demonstrate the relationship between them. The IOP elevated significantly following infection in all cases ($p = 0.001$ and $p = 0.008$ at 6 and 12 months postinfection, respectively; Wilcoxon signed-rank test) and both stage IIIa and stage IIIb ($p = 0.028$ and $p = 0.008$ at 6 and 12 months postinfection, respectively, for stage IIIa; similarly, $p = 0.002$ and $p = 0.005$ for stage IIIb). The IOP did not change in stages I and II. The number of anti-glaucoma medications used was 0.34 ± 0.71 (0–3), 0.48 ± 0.95 (0–5) and 0.45 ± 0.99 (0–5) [mean ± standard deviation (range)] for preinfection and at 6 and 12 months postinfection, respectively.

As for the associated factor analysis with poor prognosis, the multiple logistic regression analysis revealed that being stage III and having a culture positive were statistically significantly associated with the deterioration of visual acuity 12 months following the development of bleb-related infection with an increase in logMAR of at least 0.5 units (Table 6). Similarly, the multiple logistic regression analysis demonstrated that only being stage III was statistically significantly associated with IOP elevation at 12 months following the development of bleb-related infection that was defined as an increase in IOP of 5 mmHg or greater (Table 7).

As for the risk factors for being stage III, the multiple logistic regression analysis revealed that only lens status was significantly associated with being stage III and stage IIIb, but no factors were found to be associated with being stage IIIa (Table 8).

Discussion

The present study reports the visual outcome of bleb-related infection and found that the visual acuity dropped by a mean of 0.504 logMAR units at 12 months postinfection, with marked variation among the stages. Being stage III and having a positive bacterial culture were identified as significant factors for poor visual prognosis. In previous reports, the visual outcome of bleb-related infection was poor in endophthalmitis cases. For example, Busbee et al. (2004) reported in a retrospective study of 68 eyes of 68 consecutive cases of bleb-associated endophthalmitis that the incidence of no light perception was 35% at 12 months after treatment and that the incidence of visual loss, defined as at least 5 Snellen lines was 64%. In addition, they found that a positive vitreous culture was associated with significantly worse visual acuity. Song et al. (2002) identified 49 eyes of 49

Table 3. Changes in logMAR.

	Preinfection		6-month postinfection			12-month postinfection		
	Mean ± SD	*N*	Mean ± SD	*N*	p-value	Mean ± SD	*N*	p-value
Stage I	0.524 ± 0.920	61	0.538 ± 0.893	60	0.688	0.664 ± 0.997	54	0.379
Stage II	0.906 ± 1.093	23	1.380 ± 1.151	18	0.116	1.346 ± 1.277	20	0.055
Stage IIIa	0.503 ± 1.010	14	1.071 ± 1.329	10	0.036	1.602 ± 1.456	9	0.068
Stage IIIb	0.726 ± 0.862	24	1.841 ± 1.285	25	0.002	1.838 ± 1.351	24	0.003
Total cases	0.634 ± 0.955	122	1.007 ± 1.189	113	0.000	1.138 ± 1.263	107	0.000

SD = standard deviation, *N* = number of eyes, p value: versus preinfection logMAR by Wilcoxon signed-rank test including only cases where paired data were available.

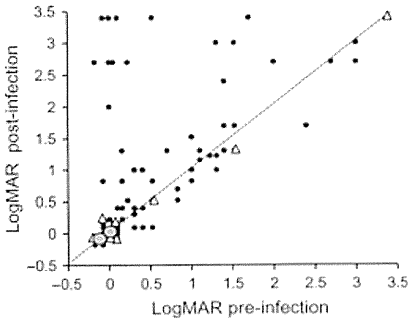

Fig. 1. Distribution of logMAR (preinfection versus 6 months postinfection). Small circles: one eye; triangles: 2–4 eyes; large circles: five eyes.

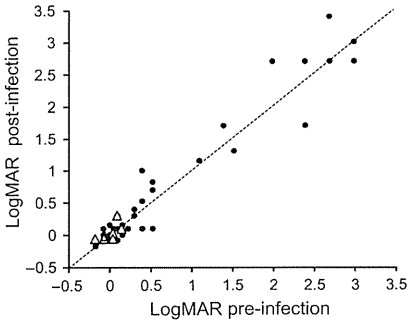

Fig. 2. Distribution of logMAR among stage I cases (preinfection versus 12 months postinfection). Circles: one eye; triangles: 2–4 eyes.

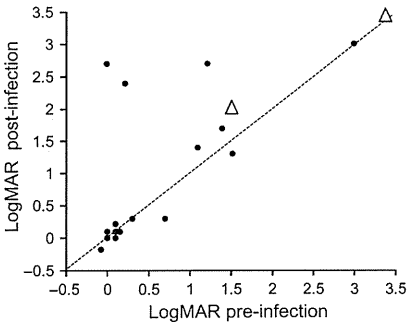

Fig. 3. Distribution of logMAR among stage II cases (preinfection versus 12 months postinfection). Circles: one eye; triangles: two eyes.

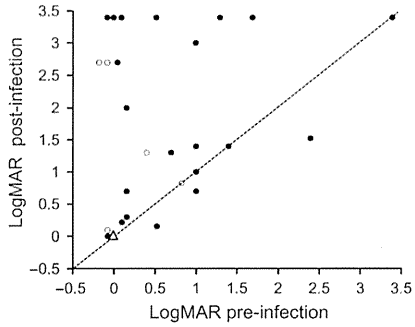

Fig. 4. Distribution of logMAR among stage III cases (preinfection versus 12 months postinfection). Open circles: 1 stage IIIa eye; closed circles: 1 stage IIIb eye; triangle: 2 stage IIIa eyes.

cases with delayed-onset bleb-associated endophthalmitis and reported that the final visual acuity was 20/40 or better in 10%, between 20/50 and 20/400 in 43% and < 5/200 in 45% of the eyes studied. The proportion of patients 20/400 or better was reported to be 47% by Kangas et al. (1997), 22% by Ciulla et al. (1997), 57% by Mandelbaum et al. (1985) and 55% by Leng et al. (2011) in bleb-associated endophthalmitis. In our series consisting of cases in which preinfection visual acuity was at least 20/40, the incidence of the ratio of visual acuity being 20/400 or better was 56% in stage III infections. Thus, the visual outcome data were similar to that reported previously for bleb-associated endophthalmitis cases. Greenfield et al. (1996) reported an average increase in logMAR of 1.42 units following bleb-related endophthalmitis and 62% showed 20/400 or better visual acuity after resolution. By contrast, Poulsen & Allingham (2000) reported much better visual outcome: 20/25 or better in each of three blebitis cases and 20/200 or better in 16 of 17 endophthalmitis cases. The mean increase in log MAR was 0.140, 0.440, 1.099 and 1.122 at 12 months postinfection for stage I, II, IIIa and IIIb infections, respectively, in the present study. Hence, our outcome data did not represent an improvement over those from previous reports on both blebitis and endophthalmitis. Even in this modern age of sophisticated technology including vitreoretinal surgery and anti-bacterial medications, bleb-related infection still posed a significant threat to visual acuity.

We also demonstrated that IOP did not change in stages I and II, and that it increased by a mean of 2.7 and 6.6 mmHg at 12 months postinfection for stage IIIa and IIIb, respectively, In addition, being stage III was again a significant risk factor for increased IOP. Thus, bleb-related infection did affect IOP control and this was especially the case in stage III infections. Previously, Song et al. (2002) focused on IOP outcomes in bleb-related infections and reported that the IOP

Table 4. Visual acuity at the final follow-up for cases in which preinfection visual acuity was at least 20/40.

Stage	20/40 or better	20/50 to 20/400	Worse than 20/400
I	36/38 (95%)	2/38 (5%)	0/38 (0%)
II	8/12 (67%)	1/12 (8%)	3/12 (25%)
III	7/18 (39%)	3/18 (17%)	8/18 (44%)
IIIa	5/8 (63%)	0/8 (0%)	3/8 (38%)
IIIb	2/10 (20%)	3/10 (30%)	5/10 (50%)
Total cases	51/68 (75%)	6/68 (9%)	11/68 (16%)

Table 5. Changes in intraocular pressure (mmHg).

	Preinfection		6-month postinfection			12-month postinfection		
	Mean ± SD (range)	*N*	Mean ± SD (range)	*N*	p-value	Mean ± SD (range)	*N*	p-value
Stage I	10.3 ± 3.9 (4–27)	70	11.0 ± 4.5 (4–26)	68	0.062	11.2 ± 3.9 (2–22)	57	0.207
Stage II	10.6 ± 4.4 (5–24)	27	10.1 ± 4.8 (0–24)	26	0.566	10.5 ± 5.5 (0–20)	22	0.944
Stage IIIa	10.2 ± 2.7 (7–15)	15	14.6 ± 5.7 (7–22)	10	0.028	12.9 ± 8.2 (0–24)	8	0.008
Stage IIIb	8.6 ± 3.8 (2–16)	30	13.3 ± 5.0 (3–21)	19	0.002	15.2 ± 6.5 (8–33)	15	0.005
Total cases	9.9 ± 3.8 (2–27)	142	11.5 ± 4.9 (0–26)	126	0.000	11.8 ± 5.2 (0–33)	102	0.008

SD = standard deviation, *N* = number of eyes. p-value: versus preinfection intra-ocular pressure by Wilcoxon signed-rank test including only cases where paired data were available.

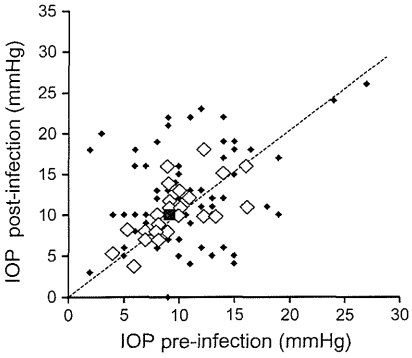

Fig. 5. Distribution of intra-ocular pressure (preinfection versus 6 months postinfection). Small diamonds: one eye; large diamonds: 2–4 eyes; large square: five eyes.

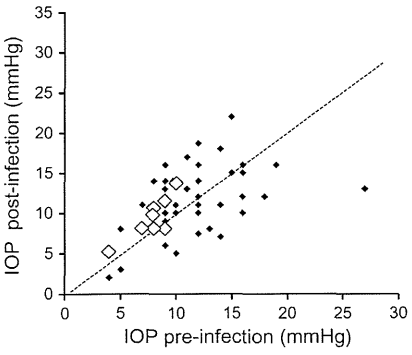

Fig. 6. Distribution of intra-ocular pressure among stage I cases (preinfection versus 12 months postinfection). Small diamonds: one eye; large diamonds: 2–4 eyes.

was uncontrolled (>21 mmHg) in 11% of such cases. Chen et al. (1997) stated that 11 of 12 bleb infections were associated with good IOP control after the resolution of the infection in an outpatient sample. Greenfield et al. (1996) reported a mean IOP increase of 1.2 mmHg following endophthalmitis. Thus, the IOP outcome findings in the present study were consistent with those of previous reports.

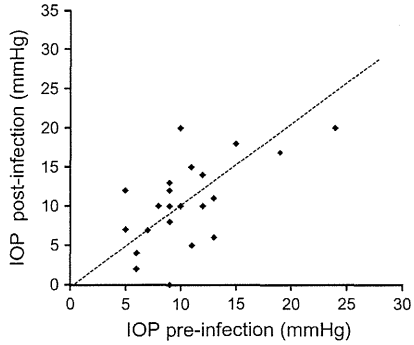

Fig. 7. Distribution of intra-ocular pressure among stage II cases (preinfection versus 12 months postinfection). Small diamonds: one eye.

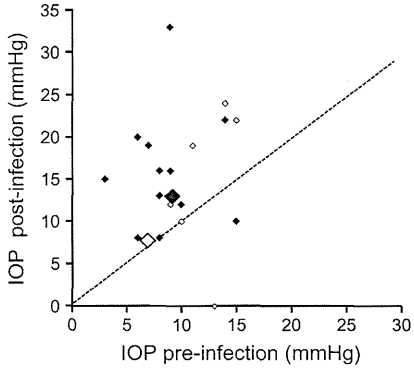

Fig. 8. Distribution of intra-ocular pressure among stage III cases (preinfection versus 12 months postinfection). Open diamonds: stage IIIa; closed diamonds: stage IIIb; small diamonds: one eye; large diamonds: two eyes.

The present study identified that being stage III infection was a significant prognostic factor for both poor visual acuity and increased IOP. Positive bacterial culture was also associated with poor visual acuity. Other factors such as age, gender, interval between surgery and development of infection, history of bleb leakage, type of conjunctival incision and preinfection IOP were not associated with a poor prognosis. The prognostic factors were apparently different from those related to the development of the infection. The latter included history of bleb leakage, use of antimetabolites, inferiorly located bleb, avascular bleb and history of diabetes mellitus (Soltau et al. 2000; Jampel et al. 2001; Matsuo et al. 2002; Hori et al. 2009).

We found that aphakia or pseudophakia was significantly associated with the development of a stage III or stage IIIb bleb-related infection, which was consistent with previous reports. Ciulla et al. (1997) identified 10 blebitis and 26 late endophthalmitis cases; six cases (60%) were phakic in the former, whereas 20 cases (77%) had prior cataract surgery in the latter series. In a series of cases reported by Poulsen & Allingham (2000), 12 cases (71%) of endophthalmitis after glaucoma filtering surgery were pseudophakic. A possible interpretation of our result in light of these previous reports (Ciulla et al. 1997; Poulsen & Allingham 2000) is that once the causative agents enter into the eyeball, they can swiftly invade into the vitreous in pseudophakic or aphakic eyes. Another important finding in the present study is that stage III bleb-related infection has significantly worse visual prognosis and poorer IOP control, which is consistent with previous reports (Ciulla et al. 1997; Song et al. 2002; Busbee et al. 2004). Some stage III infections develop quite rapidly and can even reach stage IIIb within 24 hr. Thus, patient education is essential, particularly in pseudophakic or aphakic cases, with special emphasis on attention to the early signs and symptoms of bleb-related infection. In addition, the use of antibiotics for emergencies should be emphasized to all patients with a functioning bleb,

Table 6. Results of the multiple logistic regression analysis for 0.5 unit change in logMAR.

Variable	Value	Odds ratio	95% Confidence interval	p-value
Stage III	Yes	9.26	2.03–26.53	0.002
	No	1		
Culture	Positive	6.29	1.50–26.40	0.012
	Negative	1		

Factors not significantly associated: age, gender, interval between surgery and development of infection, detection of *Streptococcus* species, history of bleb leakage, type of conjunctival incision, and preinfection intra-ocular pressure.

Table 7. Results of the multiple logistic regression analysis for intra-ocular pressure (IOP) elevation of 5 mmHg or greater.

Variable	Value	Odds ratio	95% Confidence interval	p-value
Stage III	Yes	8.33	2.51–27.71	0.001
	No	1		

Factors not significantly associated: age, gender, interval between surgery and development of infection, detection of bacteria, detection of *Streptococcus* species, history of bleb leakage, type of conjunctival incision, and preinfection IOP.

Table 8. Results of the multiple logistic regression analysis for associated factors with stage III.

Variable	Value	Odds ratio	95% Confidence interval	p-value
For stage III				
Lens status	Pseudophakic/Aphakic	2.85	1.22–6.66	0.015
	Phakic	1		
For stage IIIb				
Lens status	Pseudophakic/Aphakic	6.30	2.32–17.13	0.000
	Phakic	1		

Factors not significantly associated: age, gender, interval between surgery and development of infection, detection of bacteria, detection of *Streptococcus* species, history of bleb leakage, type of conjunctival incision, and preinfection intra-ocular pressure.

including in cases with pseudophakia or aphakia.

As previously reported (Yamamoto et al. 2012), the lack of a predetermined protocol for both treatment and bacterial culture is a major limitation to the present study. Certain missing data during the follow-up period have rendered some of our conclusions more tentative. In addition, this study was conducted in a particular region of the world and may not be generalizable to other populations. However, we believe that the results obtained are still relevant due to the large number of cases analyzed and are useful in determining the indication for trabeculectomy.

One of the most striking results of this collaborative study was that severe visual disturbance resulted in many cases following development of bleb-related infection. The proportion of 20/400 or less was 16% in eyes in which preinfection visual acuity was at least 20/40. Some of them were enucleated or ended up with phthisis bulbi. We should warn both patients and ophthalmologists against this sight-threatening complication. It is recommended to prescribe antibiotics in advance and ask the patients to administer it if they notice some symptoms of infection. Conjunctival hyperemia or conjunctivitis in eyes with a history of glaucoma filtration surgery should be treated as a medical emergency. Leaking blebs should be surgically treated before they become infected. Prevention, early detection and treatment are highly desirable to prevent severe visual loss caused by bleb-related infection from occurring.

The present study clearly indicates that the earlier the stage of the infection, the better the prognosis. Severe visual impairment is inevitable in some stage III infections and preventative measures are required to reduce the visual compromise caused by bleb-related infection, especially in pseudophakic or aphakic cases. Early consultation and treatment and thorough patient education are clearly essential to ensure the best prognosis in bleb-related infection. The JGSSBI has revealed important characteristics, outcomes and prognostic factors of bleb-related infections which have been reported here and in our previous report (Yamamoto et al. 2012). It is our hope that these findings will be of practical benefit to both practitioners and our patients.

Acknowledgments

The authors have no proprietary interest in the material described in this manuscript. The researcher list of the JGSSBI is available on the homepage of Acta Ophthalmologica related to a paper listed in the reference (Yamamoto et al. 2012).

References

Azuara-Branco A & Katz LJ (1998): Dysfunctional filtering blebs. Surv Ophthalmol **43**: 93–126.

Busbee BG, Recchia FM, Kaiser R, Nagra P, Rosenblatt B & Pearlman RB (2004): Bleb-associated endophthalmitis. Clinical characteristics and visual outcomes. Ophthalmology **111**: 1495–1503.

Chen PP, Gedde SJ, Budenz DL & Parrish RK (1997): Outpatient treatment of bleb infection. Arch Ophthalmol **115**: 1124–1128.

Ciulla TA, Beck AD, Topping TM & Baker AS (1997): Blebitis, early endophthalmitis and late endophthalmitis after glaucoma-filtering surgery. Ophthalmology **104**: 986–995.

DeBry PW, Perkins TW, Heatley G, Kaufman P & Brumback LC (2002): Incidence of late-onset bleb-related complications following trabeculectomy with mitomycin. Arch Ophthalmol **120**: 297–300.

Greenfield DS (1998): Bleb-related ocular infection. J Glaucoma **7**: 132–136.

Greenfield DS, Suñer IJ, Miller MP, Kangas TA, Palmberg PF & Flynn HW Jr (1996): Endophthalmitis after filtering surgery with mitomycin. Arch Ophthalmol **114**: 943–949.

Hori N, Mochizuki K, Ishida K, Yamamoto T & Mikamo H (2009): Clinical characteristics and risk factors of glaucoma filtering bleb infections. J Jpn Ophthalmol Soc **113**: 951–963.

Jampel HD, Quigley HA, Kerrigan-Baumrind LA, Melia BM, Friedman D & Barron Y (2001): Risk factors for late-onset infection following glaucoma filtration surgery. Arch Ophthalmol **119**: 1001–1008.

Kangas TA, Greenfield DS, Flynn HW, Parrish RK & Palmberg P (1997): Delayed-onset endophthalmitis associated with

conjunctival filtering blebs. Ophthalmology **104**: 746–752.

Katz LJ, Cantor LB & Spaeth GL (1985): Complications of surgery in glaucoma: early and late bacterial endophthalmitis following glaucoma filtering surgery. Ophthalmology **92**: 959–963.

Leng T, Miller D, Flynn HW Jr, Jacobs DJ & Gedde SJ (2011): Delayed-onset bleb-associated endophthalmitis (1996-2008): causative organisms and visual acuity outcomes. Retina **31**: 344–352.

Mandelbaum S, Forster RK, Gelender H & Culbertson W (1985): Late onset endophthalmitis associated with filtering blebs. Ophthalmology **92**: 964–972.

Matsuo H, Tomidokoro A, Suzuki Y, Shirato S & Araie M (2002): Late-onset transconjunctival oozing and point leak of aqueous humor from filtering bleb after trabeculectomy. Am J Ophthalmol **133**: 456–462.

Mochizuki K, Jikihara S, Ando Y, Hori N, Yamamoto T & Kitazawa Y (1997): Incidence of delayed onset infection after trabeculectomy with adjunctive mitomycin C or 5-fluorouracil treatment. Br J Ophthalmol **81**: 877–883.

Poulsen EJ & Allingham RR (2000): Characteristics and risk factors of infections after glaucoma filtering surgery. J Glaucoma **9**: 438–443.

Rai P, Kotecha A, Kaltsos K, Ruddle JB, Murdoch IE, Bunce C & Barton K (2012): Changing trends in the incidence of bleb-related infection in trabeculectomy. Br J Ophthalmol **96**: 971–975.

Sharan S, Trope GE, Chipman M & Buys YM (2009): Late-onset bleb infections: prevalence and risk factors. Can J Ophthalmol **44**: 279–283.

Shigeeda T, Tomidokoro A, Chen YN, Shirato S & Araie M (2006): Long-term follow-up of initial trabeculectomy with mitomycin C for primary open-angle glaucoma in Japanese patients. J Glaucoma **15**: 195–199.

Soltau JB, Rothman RF, Budenz DL, Greenfield DS, Feuer W, Liebmann JM & Ritch R (2000): Risk factors for glaucoma filtering bleb infections. Arch Ophthalmol **118**: 338–342.

Song A, Scott IU, Flynn HW & Budenz DL (2002): Delayed-onset bleb-associated endophthalmitis: clinical features and visual acuity outcomes. Ophthalmology **109**: 985–991.

Waheed S, Ritterband DC, Greenfield DS, Liebmann JM, Seedor JA & Ritch R (1998): New patterns of infecting organisms in late bleb-related endophthalmitis: a ten year review. Eye **12**: 910–915.

Yamamoto T, Kuwayama Y & The Collaborative Bleb-related Infection Incidence and Treatment Study Group (2011): Interim clinical outcomes in the Collaborative Bleb-related Infection Incidence and Treatment Study. Ophthalmology **118**: 453–458.

Yamamoto T, Kuwayama Y, Kano K, Sawada A & Shoji N & The Study Group for the Japan Glaucoma Society Survey of Bleb-related Infection (2012): Clinical features of bleb-related infection: a 5-year survey in Japan. Acta Ophthalmol [Epub ahead of print].

Received on August 7th, 2012.
Accepted on December 4th, 2012.

Correspondence:
Tetsuya Yamamoto, MD, PhD
Department of Ophthalmology
Gifu University Graduate School of Medicine
1-1 Yanagido
Gifu-shi 501-1194
Japan
Tel: + 81 58 230 6283 or 6284
Fax: + 81 58 230 6285
Email: mmc-gif@umin.net